Title
Quantitative electrophysiology as a biomarker of Autism Spectrum Disorder

Author
McEvoy, Kevin

Publication Date
2014

Peer reviewed|Thesis/dissertation

UNIVERSITY OF CALIFORNIA

Los Angeles

Quantitative electrophysiology as a biomarker of Autism Spectrum Disorder

A dissertation submitted in partial satisfaction

of the requirements for the degree

Doctor of Philosophy in Neuroscience

by

Kevin Anthony McEvoy

2015

ABSTRACT OF THE DISSERTATION

Quantitative electrophysiology as a biomarker of Autism Spectrum Disorder

by

Kevin Anthony McEvoy

Doctor of Philosophy in Neuroscience

University of California, Los Angeles, 2014

Professor Shafali S. Jeste, Chair

Autism Spectrum Disorders (ASD) are a collection of neurodevelopmental disorders with features of impairments in two domains: social communication, and restrictive repetitive behaviors/interests. Quantitative electroencephalography (QEEG) holds promise as a translational method for investigating abnormal neural oscillatory activity in ASD. Use of QEEG in ASD research is increasing, however discrepancies exist among the types of methods, artifact handling, and analyses researchers use. To facilitate comparing results across researchers, a solid foundation for use of QEEG in ASD research is needed. This dissertation builds a framework for using QEEG in future studies on children with ASD through a detailed description of data processing, artifact effects, statistical analysis methods, and differences in QEEG measures between children with ASD and typically developing controls. Chapter 2 presents a systematic approach to establishing clean, artifact-free data, and investigates the effect of artifacts on QEEG band power measures in children. We demonstrate that: (1) data quality is similar between a diverse group of children with ASD and a control group of typically developing children (TD), and (2) group differences in QEEG measures are not confounded by group differences in artifacts. Chapter 3 focuses on incorporating individual diversity observed in ASD into frequency band

power analyses. It first demonstrates the need for including phenotypic information in QEEG analyses, and then describes frequency band power differences between typically developing children and children with ASD.

The dissertation of Kevin Anthony McEvoy is approved.

Mirella Dapretto

Andrew F. Leuchter

Peyman Golshani

Shafali S. Jeste, Committee Chair

University of California, Los Angeles

2015

Dedicated to Brian and Joan McEvoy

Table of Contents

List of Figures

List of Tables

ACKNOWLEDGEMENTS

This work would not have been possible without the help of my family and friends. I would particularly like to thank my parents, Brian & Joan, and my siblings, AnneMarie, Brian, & Darin for their endless support and encouragement.

My training has been supported by the following grants: Medical Scientist Training Program (National Institute of General Medical Scientists (NIGMS), T32 GM008042-32S1), National Institute of Mental Health (K23 MH094517), Autism Speaks Weatherstone Fellowship (7845), and UCLA's Heyler Research Award. I also with to thank UCLA's David Geffen School of Medicine, the Neuroscience Interdepartmental Program, and the Center for Autism Research and Treatment for their generous support,

Chapter 2 is a version of: McEvoy K, Hasenstab K, Senturk D, Sanders A, Jeste SS. Physiologic artifacts in the resting state EEG of young children: Methodological considerations for noisy data. In: Brain Imaging and Behavior. Springer, In press.

Vita

2003-2005	Undergraduate researcher, D'Esposito Lab, UC Berkeley
2005	B.A. (Cognitive Science, Highest Honors) and B.A. (Molecular and Cell Biology), UC Berkeley
2005-2006	Research Assistant, Gazzaley Lab, UC San Francisco
2009	Neuroimaging Training Program, UCLA
2012-2014	Weatherstone Fellow, Autism Speaks

PUBLICATIONS

McEvoy K, Hasenstab K, Senturk D, Sanders AJ, Jeste SS. Physiologic artifacts in resting state EEG of young children: methodological considerations for noisy data. Brain Imaging and Behavior (In Press).

Hasenstab K, Sugar C, Telesca D, McEvoy K, Jeste SS, Senturk D. Identifying longitudinal trends within EEG experiments. Biometrics (Submitted).

Reches A, Laufer I, Ziv K, Cukierman G, McEvoy K, Ettinger M, Knight RT, Gazzaley A, Geva AB. Network dynamics predict improvement in working memory performance following donepezil administration in healthy young adults. Neuroimage (Nov 2013). 88(0): 228-241.

Gazzaley A, Clapp W, Kelley J, McEvoy K, Knight RT, D'Esposito M. Age-related top-down suppression deficit in the early stages of cortical visual memory processing. PNAS (Sept 2008). 105(35): 13122-6.

Gazzaley A, Cooney JW, McEvoy K, Knight RT, D'Esposito M. Top-down enhancement and suppression of the magnitude and speed of neural activity. J Cogn Neurosci. Mar;17(3):507-17. 2005

ABSTRACTS

McEvoy K, Jeste SS. Correlations of Quantitative EEG with Language and Cognitive Functioning As Biomarkers of Autism Spectrum Disorders. Presented at the International Meeting for Autism Research. Atlanta, Georgia. 2014.

McEvoy K, Jeste SS. Methodological considerations for processing quantitative EEG data in children with and without a developmental disability. Society for Neuroscience. San Diego, California. 2013

McEvoy K, Jeste SS. High frequency oscillations serve as a promising biomarker of autism spectrum disorders (ASD). Child Neurology Society. Austin, Texas, 2013.

McEvoy K, Jeste S. Comparison and Recommendations for Processing EEG Data in Children with Autism and Typical Developing Controls. Presented at the International Meeting for Autism Research, San Sebastian, Spain, 2013

McEvoy K, Noroña A, Shimizu C, Jeste S. Resting-State Gamma Power in Young Children with ASD Participating in a Treatment Program. Presented at International Meeting for Autism Research, Toronto, Canada, 2012

Noroña A, McEvoy K, Shimizu C, Hutman T, Jeste S. Resting-State Gamma Power and Early Language Function in Infants at Risk for Autism. Presented at International Meeting for Autism Research, Toronto, Canada, 2012

Noroña A, McEvoy K, Hutman T, Johnson S, Jeste S. Visual Statistical Learning in Infants at Risk for ASD. Presented at International Meeting for Autism Research, San Diego, CA 2011.

Jeste S, McEvoy K, Noroña A, Paparella T, Freeman S. Neural Correlates of Implicit Learning in Young Children with ASD. Presented at International Meeting for Autism Research, San Diego, CA 2011.

McEvoy K, Gazzaley A, Azevedo A, Knight RT, D'Esposito M. Top-down modulation of early and late induced gamma oscillations during working memory. Presented at The Society for Neuroscience, Washington, DC, 2005.

Miller BT, Gazzaley A, McEvoy K, Knight RT, D'Esposito M. Functional Deactivation of the Prefrontal Cortex Disrupts Posterior Physiological Signals: Joint TMS/EEG Evidence for PFC-mediated Top-Down Modulation. Presented at The Society for Neuroscience, Washington, DC, 2005.

Kelley JB, Gazzaley A, McEvoy K, Knight RT, D'Esposito M. Top-Down Modulation Deficit of the P300 in Normal Aging. Presented at The Society for Neuroscience, Washington, DC, 2005.

McEvoy K, Gazzaley A, Kelly J, Knight RT, D'Esposito M. "Age-related Impairment in Top-Down Modulation of Visual Processing: ERP Evidence." Presented at The Society for Neuroscience, San Diego, CA, 2004.

Gazzaley A, McEvoy K, Cooney JW, Kelly J, Knight RT, D'Esposito M. "Top-down modulation of Visual Association Cortex: Converging fMRI and ERP evidence." Presented at The Cognitive Neuroscience Society, San Francisco, CA, 2004.

Chapter 1: Introduction

1.1 Autism Spectrum Disorders

Autism Spectrum Disorders (ASD) are a collection of neurodevelopmental disorders with features of impairments in two domains: social communication, and restrictive repetitive behaviors/interests (American Psychiatric Association, 2013). The most recent reports from the CDC show that prevalence estimates continue to increase, and currently an estimated 1 in 68 children has an ASD (1 in 42 boys; 1 in 189 girls). Regardless of the reason for the increased prevalence, there is a need for more research for accurate diagnosis, optimal treatment, and the pathophysiology of the disorder. Given that early diagnosis improves long term outcome (Lord, 1995) (Rodgers, 1996), it is essential to improve early diagnosis. Despite the fact that reliable diagnosis can be made by the age of 24 months (Kleinman et al., 2008; Lord et al., 2006), the most recent CDC reports indicate the median age at which diagnosis is made is not until 53 months of age (CDC ADDM Network, 2014).

Delayed language acquisition is a common indicator of the disorder, and the absence of first words or phrases is the most common initial concern reported by caregivers of children with ASD (Wetherby et al. 2004). While early language function is a key prognostic factor for individuals with ASD (Lord and Ventner 1992), the heterogeneity in language outcomes remains exceptionally large, with estimates of 30% to 50% remaining nonverbal (Anderson et al. 2007; Tager-Flusberg and Kasari, 2013). Language abnormalities range from impaired pragmatics, to difficulties with syntax and semantics, to phonological processing deficits (Groen et al. 2008).

Behavioral measures have been successful at characterizing various levels of verbal abilities, but because they can only capture overt behaviors, they unfortunately struggle to subtype children with similar language levels. For example, they are unable to differentiate preverbal from nonverbal children. In addition, behavioral measures alone cannot address the underlying neural mechanisms and pathways that underlie the deficits and delays of language impairment. Innovative use of physiologic measures and translational methods are therefore required to provide insight into biologic processes of language function in ASD.

A current approach to understanding these processes is through identification of biomarkers, or objectively quantifiable indicators of biologic states. One physiologic measure that has shown promise in other developmental and adult neuropsychiatric disorders is through measurement of neural activity as recorded by electroencephalography (EEG). As a biomarker, quantitative EEG (QEEG) is a measure of neural oscillatory activity while an individual is at rest or engaged in a task. Research has demonstrated it is effective in suggesting optimal treatments (Leuchter et al., 2009), early disorder detection (Bosl, Tierney, Tager-Flusberg, & Nelson, 2011), identifying subgroups within a disorder (Clarke et al., 2011), monitoring treatment outcomes (Dawson et al., 2012), monitoring typical brain function over development (Marshall, Bar-Haim, & Fox, 2002), and even predicting functional outcomes (Gou, Choudhury, & Benasich, 2011). The utility of QEEG is not limited to these clinical applications. As a measure more proximal to the source of deficits in ASD, it can also provide insight into pathways to language impairment in ASD. Even though a relatively small number of studies have used QEEG to examine ASD, the findings suggest several ways it could be useful as a biomarker of the disorder. However, because of differences between methods, questions asked, and even subject populations, the results of these

studies often appear to conflict. If QEEG can be used as a biomarker for ASD, an initial framework of QEEG measures in ASD needs to be established.

1.2 Quantitative Electroencephalography

Uses

Quantitative EEG measures neural oscillatory activity primarily related to postsynaptic activity in the neocortex. Its main clinical use is in characterizing epileptiform and seizure activity, the risk of which is increased in ASD (Tuchman & Rapin 1997, 2002). It is also used to study sleep disturbances, where the incidence is also increased in ASD (Chez et al., 2006). As a research tool, QEEG has a well-established history for studying neural activity in typically developing children (Marshall, Fox, etc.) and neurotypical adults (Basar, Basar-Eroglu, Karakas, & Schurmann, 2001), as well as in neuropsychiatric disorders such as depression (Cook & Leuchter, 2001; Loo et al., 2009), schizophrenia , and ADHD (Loo et al., 2009; Uhlhaas & Singer, 2010).

Advantages

The exquisite millisecond temporal resolution of the recordings make EEG well suited to studying precise timing differences in neural activity between different groups or experimental manipulations. Consequently, the majority of experimental EEG research looks at time-locked, event related changes in the amplitude or latency of recorded neural electric activity, so-called event-related potentials (ERP). By averaging the time-locked signal over many repetitions of the same event, this method enhances the signal related to a specific event, while removing what is often thought of merely as background “noise.” However, this ongoing background activity is far from being noise. Many studies have demonstrated that EEG activity prior to an event predicts

subsequent ERP measurements (Gruber et al., 2005; Mazaheri et al., 2009). In vivo studies on animals also demonstrate the importance of on-going neural activity, for example by showing that the neuronal firing rates are affected by the rhythmic fluctuations in the electrical potential in their local environmental background, referred to as "up-and-down states." In humans, QEEG is used to study this background activity most often while subjects are at rest, but an increasing number of studies are also studying non-time locked changes in the neural activity while subjects are engaged in an activity, for example executive function tasks. An additional advantage of QEEG over event related experiments is that QEEG, by its very nature, measures ongoing neural activity without requiring sensory stimulation or overt behaviors. Not only does this allow the scientific questions to investigate neural activity in a more natural state than in time-locked, event related designs, but it is also a practical advantage because it enables studying difficult populations, for example infants and children with developmental disorders such as ASD. Compared to technologies such as fMRI or PET, QEEG has additional practical advantages of EEG, including: relatively cost effective, lower startup cost, increased availability, ease of use, and is noninvasive. Even though the scientific questions should not be driven by the practical advantages of a method, they are important considerations when searching for biomarkers with clinical utility.

Frequency Bands

Investigation of neural oscillatory activity is accomplished by first decomposing the time-varying changes of the EEG signal into a measure of how much each frequency contributes to the overall signal. Stating it differently, the signal is transformed from a measure that changes over time (i.e. time-domain) to a measure that changes over frequencies (i.e. frequency-domain). Next, the measured amount of each frequency (i.e. power) at each sequential frequency step is averaged across groups of neighboring frequencies (i.e. frequency bands) and used in statistical tests, for

example to determine how neural activity differs across hemispheres, groups, or experimental conditions. The range of frequencies within a frequency band all share physiologic properties, and research has demonstrated that power in different bands and regions of the scalp relate to various sensory and cognitive processes. The most commonly studied bands are delta (1-3 Hz), theta (4-7 Hz), alpha (8-12 Hz), beta (13-35 Hz), and gamma (>35 Hz). Delta activity is most often associated with deep sleep, but research has also suggested it plays a role in motivation, attention, and low-level processes such as salience detection and perception (Knyazev, 2012). Increased power in the theta band is associated with memory and recall (Klimesch et al., 1996). Alpha band activity is prominent over occipital scalp regions. In many adults it can be reliably induced during wakeful resting with eyes closed, which led to its interpretation as an 'idling rhythm' (Basar et al., 2000). It is commonly believed that increased alpha activity is also involved in inhibitory functions (Uhlhaas et al, 2009). The beta band is not studied as often as the other bands, but studies suggest it is involved in motor behaviors and alertness (Neuper & Pfurtscheller, 2001). In recent years, a great deal of research has focused on the gamma band because it is believed to play a role in several higher cognitive processes including language, memory, attention, and object representation (Benasich et al., 2008; Basar et al., 2000; Tallon-Baudry et al., 1999).

Power Measures

The power measure reported is most commonly based on either of two closely related calculations. The first, referred to as absolute power (measured in μV2) is the raw measure of power at each frequency averaged across all frequencies within a band. The second type of power measure, referred to as relative power, is the percentage of power within a frequency band relative to all other frequency bands, and it is simply calculated by dividing each band's absolute power by the sum of the absolute power across all frequency bands. Relative power is helpful in

standardizing absolute power differences across subjects, which may be particularly useful in studies on developmental populations because differences in skull thicknesses can have a large effect on absolute power estimates. However, because there is a known (1/f) logarithmic nature of the EEG power spectrum (Buzsaki & Draguhn, 2004), differences in relative power across frequency bands and groups may be more difficult to interpret than in absolute power.

Challenges & Artifacts

Despite the scientific and practical reasons encouraging the use of QEEG to investigate deficits and biomarkers in ASD, challenges also exist, especially when the target population includes children with a developmental disorder. Given that children with ASD, by definition, have impairments in social communication, it can be difficult for some children to remain compliant during an experiment. This can result in a decreased quantity of acquired data. The quality of the data is also affected because QEEG is susceptible to contamination by several physiologic artifacts. Of all EEG artifacts, three of the most common are due to eye blinks, horizontal eye movements (i.e. saccades), and muscle activity (electromyographic or EMG). Various methods and techniques have been developed to handle these types of artifacts in data acquired from adults, but not all are possible or applicable to data collected from children. Furthermore, the effect each of these artifacts has on measurements of band power in different scalp regions is unknown for developmental populations.

1.3 Use of QEEG in ASD Research

Compared to developmental disorders such as Attention Deficit Hyperactivity Disorder, where there is a rich literature examining neural oscillatory activity through QEEG, studies on

ASD are relatively sparse. With only a handful of reported studies, it is not surprising that conflicting results are found across researchers. Two recent reviews provide excellent summaries of published results (Billeci et al. 2013; Wang et al. 2013), and discuss potential reasons for the mixed findings. The reasons for the mixed findings can be summarized as due to differences in: (a) the target ASD population, (b) the state of the subject during recording, and (3) the selection of outcome measures.

Target ASD Population

The ASD population studied can vary in several important ways and is particularly important because of the heterogeneity within diagnosed individuals. A finding of reduced band power reported in one study may appear to conflict with the increased band power by another study, but the characteristics of the subjects in the ASD samples are often different (e.g. age, IQ, level of impairment, etc.), as is the case with studies with studies by Cantor et al., 1986 and Mathewson et al., 2012. The study by Cantor and colleagues reported lower relative alpha power in a group of young, very impaired children with ASD (IQ = 37 ±11; Age: 4-12 yo). Mathewson and colleagues on the other hand, reported a higher relative alpha power in ASD, but subjects in the ASD sample were much higher functioning adults (IQ = 101 ±19; Age: 19-52 yo). Attempting to make conclusions regarding all individuals with ASD based on the results of these two studies is not possible. A major goal of this dissertation, is to lay a foundation built on how QEEG measures vary within the spectrum of ASD.

Subject State

Differences in what a subject is doing during an EEG recording, for example sitting at rest versus engaged in a task, contribute to conflicting results because band power measures are known to change depending on a subject's state, both cognitive and physical. Quantifying a subject's EEG

during different cognitive states allows for comparisons of neural activity at different levels of engagement and cognitive functioning, for example when a subject is at rest versus a short-term memory task. Two example studies using this approach in ASD include a "Go/No-Go" task (Chan et al., 2011), and sustained visual attention tasks (Oberman et al., 2005). The most common method for adjusting a subject's physical state during EEG recordings is to have subjects rest with eyes-closed versus eyes-open. Studies in ASD have used eyes-open (e.g. Chan et al., 2007), eyes-closed (e.g. Coben et al. 2008), and in rare occasions both eyes-open and close conditions (e.g. Pop-Jordanova et al., 2010). Recording a subject under an eyes-closed condition is beneficial because it produces a more stable (i.e. less variable) signal over time in adults and children (Corsi-Cabera, 2007; Vuga, 2008). Minimizing subject-level variability is advantageous in research questions that compare measures within the same subject, such as changes over time due to a drug or hemispheric differences. Yet when the research question is interested in group differences, then eyes-closed conditions may limit the ability to detect differences because it is more important to minimize the variability at the group-level. It has even been proposed that controlling the visual input during eyes-open conditions increases the coherent information across subjects, but in eyes-closed conditions the controlled coherent information is replaced by subject specific noise (Thuraisnigham, 2007). Reducing variability in the measure of interest (i.e. band power) across subjects is particularly important in ASD studies because of the phenotypic variability already present.

Outcome Measures

The two most commonly reported EEG measures in ASD research are of relative (e.g. Cantor et al., 1986) and absolute power (Stroganova et al., 2007). Even though these two power types are related, they are not directly comparable. When results are reported from these different

types of power measures, it is difficult to determine if the true cause of conflicting results. Other, more advanced QEEG measures are also available. In the ASD literature, some of these include coherence (Duffy & Als, 2012), phase synchronization (Thatcher et al., 2009), and multiscale entropy (Bosl et al., 2011). The complexity and diversity of these studies have provided valuable contributions, resulted in novel, interesting directions for future research, and demonstrated the benefit of QEEG research in ASD. However, they have also introduced some confusion through conflicting results. What is currently needed in the ASD literature is a reliable knowledgebase against which future QEEG measures and research can be compared.

1.4 Overview of Dissertation

This dissertation establishes a strong foundation for the use of QEEG in future studies on children with ASD through (1) a detailed description of artifact detection and effects, (2) a strategy for embracing the inherent diversity within ASD, and (3) an analysis QEEG measures in ASD across bands, scalp regions, and power types.

- Chapter 2 presents a systematic approach to establishing clean, artifact-free data, and investigates the effect of artifacts on QEEG band power measures in children. We demonstrate that: (1) data quality is similar between a diverse group of children with ASD and a control group of typically developing children (TD), and (2) group differences in QEEG measures are not confounded by group differences in artifacts. This chapter is a modified and extended version of a manuscript accepted for publication.
- Chapter 3 establishes a foundation band power measures in a diverse group of children with ASD. It starts with an investigation on the benefits of including phenotypic information in

QEEG analyses, and then uses the results to identify band power differences between typically developing children and children with ASD.

Chapter 2: Effects of Artifacts on EEG Measures

2.5 Introduction

Quantitative electroencephalography (QEEG) has served as a powerful tool to study both typical and atypical brain development and function, informing the understanding of processes such as perception, cognition, and cortical connectivity (For review see: Saby and Marshall, 2012; Uhlhaas et al., 2010). With a temporal resolution that facilitates quantification of subtle changes in state and function over time, QEEG holds tremendous promise as a quantitative biomarker of clinical phenomenon such as the change in brain function over discrete time points in development (Marshall et al., 2002), the effects of intervention in developmental disorders (Dawson et al., 2012), prediction of functional outcomes (Gou et al., 2011), early disorder detection (Bosl et al., 2011), disease progression (Luckhaus et al., 2008), and subgroup (Clarke et al., 2011) and group (Barry et al., 2010) differences in childhood psychiatric disorders. QEEG holds particular appeal as a metric of individual variability in neurodevelopmental disorders, such as autism, where behavioral output is limited and sometimes unable to capture phenotypic and functional heterogeneity (Cantor and Chabot, 2009; Saby and Marshall et al., 2012).

Scientific merits notwithstanding, it is the practical benefits of QEEG that often motivate its use in the study of developmental populations, as it is non-invasive, less vulnerable to motion artifact, and more readily available in clinical settings (Keil et al., 2014; Saby and Marshall, 2012; Webb et al., 2013). Moreover, cognitive processes such as attention, memory, cognitive inhibition, and feature binding can be characterized without requiring an overt behavioral response. However, these practical benefits also lead to greater challenges in data acquisition and quality, as the target

populations of interest (infants, young children, atypically developing children) may also generate the most artifact, resulting in an insufficient amount of useable, clean EEG data (Slifer et al., 2008; Webb et al., 2013). Unlike studies in adults where recording duration often exceed 10 minutes (Barry et al., 2007; Bonfiglio et al., 2013; Hagemann and Naumann, 2001; Leuchter et al., 2012), in infants and children a total of 2 minutes of data are often gathered, with fewer than 30 seconds of clean data remaining after artifact rejection (John et al., 1980; Marshall et al., 2002; Tierney et al., 2012).

Physiologic EEG Artifacts

Three of the most common internal sources of artifact include eye blinks, saccades, and contraction of face, jaw or neck muscles (electromyographic noise or EMG). Studies in adults have investigated techniques for handling these artifacts individually, such as independent component analysis (ICA; Jung et al., 2000) and regression methods (Gratton et al., 1983). In the study of developmental populations, ICA is often impractical because it requires substantial amounts of data (e.g. at least 10 minutes with 128 channels and a sampling rate of 500 Hz; Onton et al., 2006). When the amount of available data is already limited, there may not be enough artifacts of a given type for clear component selection (Keren, Yuval-Greenberg, and Deouell, 2010). Down sampling the number of channels (e.g. 128 to 64) is one proposed method for overcoming minimum data requirements; however, it does not necessarily make artifact related components more identifiable. Furthermore, component selection in ICA increases in difficult when multiple artifact types exist in the data. Regression methods in either the time or frequency domains can also be problematic because the regression requires removal of electrooculographic (EOG) channels that may also include relevant EEG signals along with the artifact (Jung et al., 2000). When ICA or regression methods are not possible, another traditional strategy for addressing artifacts includes the removal

of contaminated sections of data from analysis. This strategy can result in the removal of large quantities of data that may, in fact, contain valuable signal worth preserving.

Little is known about the contribution of artifacts (blinks, saccades, EMG) to the calculation of EEG power in children, despite the fact that developmental populations are the most likely to generate the highest noise:data ratio. Previous studies have provided valuable information about the effect of varying degrees of muscle contraction and its spatial spread on QEEG measurements, but these studies have included only adult subjects (Freeman et al., 2003; Goncharova et al., 2003). Finally, as has been addressed in several papers, the lack of uniformity in methods of data processing and cleaning contributes to difficulties in replicating and comparing findings (Keil et al., 2014; Picton et al., 2000; Pivik et al., 1993; Webb et al., 2013). Such a challenge holds particularly true in studies of infancy and early childhood, where no consistent parameters for data cleaning or processing have been established.

In analyses between typical and atypical populations, it is critical to measure any possible systematic differences in artifacts between groups. For instance, one might hypothesize that children with delayed development would demonstrate more eye movements or EMG artifact than typically developing children. However, studies do not consistently examine this variable in studies using QEEG. Of note, several recent studies in fMRI have shown that head motion leads to systematic biases in the analysis of functional connectivity, and that that children with autism do generate more motion artifact than typically developing controls (Deen and Pelphrey, 2012; Power et al., 2012; Satterthwaite et al., 2012; Van Dijk et al., 2012). Such a systematic bias can result in the erroneous appearance of weaker long-range connections in children with autism. These seminal studies have led to rigorous efforts for consistent motion correction in fMRI data

processing across studies and sites in studies of typical and atypical development. Similar methods will be critical with EEG artifacts in developmental populations.

Approach

We took a systematic approach to study the potential effects of artifact on EEG power in a cohort of young typically developing (TD) children and children with ASD, with the goal of guiding artifact rejection methods in EEG data processing. We focused on three common physiologic artifacts, namely blinks, saccades, and EMG, and we compared the estimation of mean spectral power within these artifacts to the mean spectral power contained in artifact-free data within characteristic frequency bands including theta (4-7 Hz), alpha (8-12 Hz), beta (13-30 Hz), and gamma (35-45 Hz). We asked whether certain power types, regions or frequency bands would be more vulnerable to the inclusion of ocular or EMG artifacts. In these main analyses, EEG from only the TD group was analyzed. As a final analysis, artifacts and their effects are compared between the TD group and the ASD group to determine if the having a developmental disorder interacts with the effects of artifacts.

2.6 Methods

2.6.1 Participants

Our research examined two groups of children: a target group of children with ASD and a control group of typically developing children (TD). There is no reason to assume that the electrophysiologic signal produced by, for example, an eye blink is different or would impact band power measures differently for children with ASD compared to TD controls. However, to avoid making this assumption, the results reported in sections 2.7.1 to 2.7.3 are based on EEG data

acquired only from the TD group. In section 2.7.4 this assumption is tested by comparing the TD and ASD groups. Therefore, a full description of both groups is given here, even though the majority of the results are from the TD group's data. Except as noted elsewhere, the details of the subjects, data acquisition, and processing provided in this methods section applies to data used in subsequent chapters as well.

For the ASD group, children were recruited from a UCLA treatment program, the Early Childhood Partial Hospitalization Program (ECPHP). ECPHP is an intensive, short-term (3 moths) day treatment program for young children (ages 2-6) diagnosed with ASD. Initial diagnosis of ASD is made by a child psychiatrist, developmental pediatricians, independent clinical psychologists, or California State Regional Center. If there is any question about the accuracy of the diagnosis, a reevaluation is performed and combines clinical history with diagnostic assessments, for example Autism Diagnostic Observation Scale (Lord et al., 1989), or Autism Diagnostic Interview-Revised (Le Couteur, Lord, Rutter, 2003).

For the TD group, children were recruited using birth records provided by Los Angeles County. Families with children in the targeted age range were mailed invitations to participate. Interested families returned a postcard and were later contacted via telephone for a screening interview. Children were excluded from the study if they had a history of neurological abnormalities, birth-related complications, developmental delays, need for special school services, uncorrected vision impairment, or a diagnosis of a psychiatric condition such as ADHD, OCD, or bipolar disorder.

A total of 114 were enrolled in the current study. The target group consisted of children with a diagnosis of ASD (n = 67), and were compared to a control group of typically developing children (TD, n = 47) (see Table 2.1). The groups did not differ in age (ASD: mean = 50.7 mo,

range =26.5 - 73.6 mo; TD: mean = 50.3, range = 24.4 – 75.2), but there was a significantly higher percentage of girls in the TD (45%, n = 21) than ASD (24%, n =16) group ($\chi^2(1) = 5.5$, $p < .05$).

Full ethical approval for the research was obtained through the University of California Institutional Review Board (IRB#:11-000355), and all parents provided written consent for the study.

2.6.2 Cognitive Assessments

On the day of the testing session, each child was assessed with the Vineland Adaptive Behavioral Scales survey (Sparrow et al., 2005), and either the Mullen Scales of Early Learning (Mullen, 1995) or Differential Abilities Scale-II (Elliott, 1993), depending on his or her age and developmental level. As part of the standardized behavioral testing performed prior to entry into ECPHP, children in the ASD were also assessed on a combination of the Wechsler Preschool and Primary Scale of Intelligence (WPPSI-IV), the Preschool Language Scale-4 (PLS-4), and the Clinical Evaluation of Language Fundamentals-4 (CELF-4; Semel, Wiig, & Secord, 2003). To facilitate comparison across assessments, only standardized scores (or t-scores converted to standard scores) were used to obtain estimates of each child's IQ, verbal IQ, non-verbal IQ, and receptive and expressive language ability. Several studies support the validity for this method of combining standard scores across cognitive assessments (Bishop, Guthrie, Coffing, & Lord, 2011; Kasari, Freeman, & Paparella, 2006). The standard scores on all cognitive assessments were significantly different between the ASD and TD groups (see Table 2.1 and Figure 2.1).

2.6.3 EEG Recording

Prior to the day of EEG recording, parents of children were asked about their child's preferences and interests, such as favorite movie or toy. This information was used on the day of the experiment to make the recording session as comfortable and enjoyable as possible for each

child. For example, children were offered a snack or shown a favorite video during placement of the EEG net.

EEG data were recorded using a 128-channel HydroCel Geodesic Sensor Net (Electrical Geodesics Inc., Eugene, OR). To improve each child's comfort, four of the electrodes, channels 125-128 had been removed from the net. These electrodes were originally located below and lateral to the eyes (Figure 2.2). Placement of electrodes conformed to the International 10-20 System (Jasper, 1958). A combination of a Net Amps 300 amplifier and Net Station 4.4.5 software on a Macintosh Pro PC was used to record the EEG (Electrical Geodesics Inc., Eugene, OR). Data were filtered online with an analog band pass elliptical filter between 0.1 to 100 Hz. The high impedance nature of this system allows us to accurately record a child's EEG while keeping impedances below 100 KΩ (Ferree et al., 2001). The EEG was sampled at 250 Hz. Data were referenced online to a vertical reference in a location equivalent to Cz. Two minutes of "resting-state" EEG was recorded while children watched a video of bouncing bubbles in a dark, sound-attenuated room. Children were either seated in a chair or on a caregiver's lap. A video time-locked to the EEG was acquired in order to assist in subsequent data processing.

2.6.4 Data Preprocessing

EEG data were processed offline through a series of steps in order to categorize segments of data by artifact: blinks, saccades, EMG, or "Other" (see Figure 2.3 for examples). Segments were categorized as "Other" if they contained drift, motion artifact because of net manipulation or pulling, or multiple artifact types. Segments that did not fall into one of these categories were determined to be clean, and hereafter are referred to as "artifact-free" segments. The full series of processing steps included the following:

(1) We applied a 1-50 Hz band-pass filter with a narrow roll-off (.3 Hz) and strong attenuation (gain = -60 dB).

(2) We segmented the data into 1.024 second sequential, non-overlapping epochs, which resulted in 256 samples per segment. The segment length was chosen to optimize inputs to the Fast Fourier Transform (FFT), which uses inputs of 2^n samples (Drongelen, 2007).

(3) We reviewed the filtered file to identify channels with gross abnormalities caused, for example, by an electrode losing contact after recording began. Channels identified as abnormal were then replaced by an interpolated signal using the Net Station software's "Bad Channel Replacement" (BCR) waveform tool, which uses spherical splines to approximate the signal from the remaining electrodes (Fletcher et al., 1996; Perrin et al., 1987; Srinivasan et al., 1996). The electrodes most commonly requiring this interpolation included those located along on the periphery of the net, either seated on the neck or surrounding the ears. No channels in our regions-of-interest (ROI) required bad channel replacement at this step (Figure 2.2).

(4) We then identified channels whose maximum to minimum voltage exceeded 150 μV within individual segments. Any segment with greater than 15% of electrodes exceeding this threshold, was placed in the "Other" category. These automated rejection criteria are based on common practices in developmental populations (for example, see Jeste et al. 2014)

(5) We manually reviewed all remaining segments and placed them into one of the five previously described categories: blinks, saccades, EMG, other, or artifact-free. A minimum of 30 seconds of clean data was required for inclusion into analysis, and this

threshold was based on prior studies in infants and young children (Marshall et al., 2002; Swingler et al., 2011; Tierney et al., 2012). Of the 32 children in the study, 2 subjects were removed from analysis because they provided fewer than 30 segments of clean data, leaving a sample of 30 children (40% girls; mean age = 53.6 mo; SD = 13.3 mo).

(6) Segments underwent an additional BCR operation. In contrast to the first BCR, which replaced a channel's data for the entire recording, this step was performed on a segment-by-segment basis. Per segment, data were interpolated for a maximum of 18 channels (15% of the 124 channels).

The final processing steps before spectral decomposition and frequency band power calculations included (7) baseline correction, (8) re-referencing to the average of all channels, (9) export of Net Station data to Matlab (Mathworks Inc., Natick, MA) and then (10) removal of each segment's DC trend using Matlab's DETREND function.

2.6.5 Artifact Detection Strategies

Several strategies, described below, were used to aid in artifact detection. The most effective strategy (#1 below) was the traditional method of correlating the expected electrophysiologic signal produced by an artifact with its expected spatial location. This method sometimes leads to missed artifact selection. Therefore other strategies were also employed, as listed below. The strategies listed below are not mutually exclusive. They were used in combination to guide decision making during artifact detection. Finally, when no clear segment categorization could be made using all available resources and strategies, segments were categorized as "Other." The purpose in detailing each of these strategies is to promote transparency

in artifact detection, and provide methods that can be shared across researchers to foster collaborative efforts. The strategies employed include:

1. *Spatial location*: An electrode's scalp location was used to identify and distinguish artifacts. For example, the electrophysiological signal produced by blinks should be maximal in electrodes located above the eyes, whereas the signal from saccades should be maximal in lateralized frontal electrodes, with opposite polarities on the left and right. However, we observed several variations of this pattern. For example, the signal produced by a saccade for some individuals only appeared in electrodes ipsilateral to the individual's gaze. Similarly, some individuals would demonstrate a saccade simultaneous to a blink, producing a combined artifact that was more challenging to identify or quantify.
2. *Re-referencing*: Temporarily switching the reference electrode within a segment helped to localize the source of an artifact. For example, switching to an average reference of all electrodes can help identify movement artifacts, whereas an average reference of all electrodes outside of the default reference can help identify a poor reference electrode in otherwise clean data. Also, referencing data as linked, bipolar pairs, can be used to enhance the visualization of eye movements.
3. *Filters*: Temporary filters can be used to minimize the signal from neural or other sources, while maximizing signals from the artifact in question. For instance, a 1-6 Hz band-pass filter can enhance the visualization of the signal from eye movements by smoothing out a distracting signal from faster sources, such as muscle or alpha generators. Similarly, a high pass filter (e.g. > 20 Hz) can help to distinguish EMG independent of, or related to blink/saccades.

4. *Topologic spectral maps*: By combining techniques (1) and (3), this strategy relies on the anatomical location of a signal generator and the characteristic frequency band of an artifact's signal. For example, the signal generated by EMG should be maximal in electrodes adjacent to muscles and an EMG signal should increase power in frequencies above 20 Hz (i.e. beta and gamma bands).
5. *Current source density*: Calculating the surface Laplacian within a segment enhances information that is maximally specific to each electrode relative to its closest neighbors. Since the surface Laplacian is the second order spatial derivative, this method acts as a spatial band-pass filter that removes shared information. As such, it represents a reference-free method that enhances signals from superficial sources, while minimizing shared signals originating from deeper neuronal sources (Nunez and Srinivasan 2006). This technique can help to identify artifacts that are channel specific (e.g. channel pops) from artifacts whose signal spreads across electrodes (e.g. EMG).

After segment categorization, EEG data from all subjects who provided a minimum of 30 artifact-free segments were kept in subsequent analysis. This resulted in final sample sizes of 54 for the ASD group (girls = 20%; mean age = 50.8 mo; SD = 13.6 mo) and 42 for the TD group (girls = 48%; mean age = 51.9 mo; SD = 14.4 mo) (see Table 2.2). The number of subjects that were removed from further analysis due to an insufficient amount of artifact-free data was not significantly different ($\chi^2(1) = 1.6$, ns) between the ASD (n = 13) and TD (n = 5) groups.

2.6.6 Constant EMG

During the manual detection of artifacts, the signal in a small number of channels for some subjects appeared to contain low amplitude EMG that was constant throughout the recording.

Using the previously mentioned strategies, further investigation determined this signal to be a form of muscle related artifact entirely separate from what is classically thought of as EMG, for example the rhythmic, large amplitude signal produced by chewing. This low amplitude, constant EMG (referred to hereafter as constant EMG) was most often observed in channels whose electrode locations corresponded to the periphery of the EEG net, especially the forehead. Additional analyses of the power spectrum of the signal recorded by these electrodes indicated the oscillatory activity recorded by these electrodes was extremely different than that of all other electrodes within the same individual. By watching video time-locked to the EEG recording, it appeared that this constant EMG artifact may be due to the EEG net slightly stretching the skin away from a completely relaxed state, which resulted in small, localized muscle contractions. This is supported by observations of the constant EMG artifact disappearing after, for example, a subject scratching his or her forehead in the region of the artifact. The constant EMG was not related to a subject's state. In fact, several subjects whose data appeared to contain this artifact sat quietly at rest throughout the entire recording, and the signal recorded in other channels was artifact-free. Despite this, data contaminated by this constant EMG could not be included in analysis. However, rather than simply removing all data from children with this artifact, only the data regions or channels affected by constant EMG were removed. A strategy was developed to determine which channels or regions should have data removed without bias. This strategy included heuristics to visually identify potential contamination by constant EMG, and subsequent statistical tests as confirmation. Full details of this strategy are described in the supplementary materials.

Statistically speaking, removal of data for specific regions from the analysis means that these subjects provided incomplete or unbalanced data. This prevents the use of certain statistical tests, as discussed in chapter 3. For the current chapter however, the analysis on the effects of

artifacts was limited to the EEG data acquired from children with complete data for all ROIs. Therefore, all EEG data included in the current analysis (TD subjects only) did not contain constant EMG, and the resultant sample size included 32 children ages 2 – 6 years old (40% girls; mean age = 52.9 mo.; SD = 13.7 mo). See Table 2.3 for the number of subjects with constant EMG by region

2.6.7 Spectral power calculations

We investigated frequency band power for 9 regions-of-interest (ROI; Figure 2.2). Regions were selected so that left, midline, and right portions of frontal, central, and posterior scalp were represented during analysis. Each region contained data from four electrodes, except for the midline-central region which contained five. We calculated estimates of the mean power spectral densities (PSD) separately for each artifact type (blinks, saccades, EMG) and for the artifact-free data. Due to the variability in the type of data in the "other" category, we did not include segments categorized as "other" in our analysis. Table 2.2 provides details on the number of segments per category.

Transformation of the EEG signal from the time-domain to the frequency-domain was accomplished using Welch's method and custom scripts written in Matlab. For each 256-sample segment, FFTs were calculated on 128-point Hamming windows with 50% overlap, yielding a frequency resolution of 0.5 Hz. We calculated absolute and relative power for the theta (4-7 Hz), alpha (8-12 Hz), beta (13-30 Hz), and gamma (35-45 Hz) frequency bands. Absolute power was calculated by summing power estimates at every 0.5 Hz increment within each frequency band. Relative power represents the power contained within a frequency band relative to the total power contained in all bands. As such, we calculated relative power by dividing the absolute power for each band by the total absolute power across all unfiltered frequencies, specifically 1-50 Hz. By

averaging across all electrodes within each ROI, final power values used for statistical analysis were obtained for each segment, within each category, and for each subject. Values for all power estimates were log transformed to achieve normality.

2.6.8 Statistical Analysis

Analysis was focused on the log-transformed absolute and relative power estimates of theta, alpha, beta, and gamma bands. As a preliminary analysis to investigate time trends across the 2 minute recording, we plotted all subject-specific response trajectories versus time segments per power band, and fitted population loess smooths. Both population and subject level smooths did not indicate a time trend. However, differences in subject-specific intercepts were apparent. The eight (4 Bands * 2 Power Types) log-power bands were modeled with a linear mixed model (LMM) using artifact type, region, and their interaction as predictors. To test that the results were not due to age, a subsequent analysis included predictors for age and an age*artifact interaction. While these additional predictors were significant for some bands, the results did not change. Since the focus of this manuscript is on the effects of artifacts, not age, results are reported only for the simplified model. A random intercept was included (using SAS PROC MIXED) to account for subject-specific heterogeneity observed in the temporal loess smooths (SAS Institute, Cary, NC). In addition to accounting for within-subject correlations, the LMM allows for unequal numbers of repetitions among subjects. In other words, the LMM controls for different number of segments per category both within (e.g. Subject A: $N_{artifact\text{-}free} = 75$, $N_{Blink} = 10$) and between subjects (e.g. Subject B: $N_{artifact\text{-}free} = 50$, $N_{Blink} = 40$). Such modeling allowed for the determination of mean power in artifact and artifact-free segments independent of the amount of data in a given subject. Mean band powers from the artifact- free category and each of the 3 artifact categories were compared for each of the 9 regions and all 8 power bands (using LSMEANS), amounting to 27

tests per model. We have adjusted using SAS PROC MULTITEST for multiple testing in all models (216 tests) controlling the false discovery rate (FDR).

2.7 Results

In sections 2.7.1 through 2.7.3, we present results as comparisons between the mean relative and absolute power for artifact-contaminated and artifact-free segments within each frequency band of interest for typically developing (TD) children. In 2.7.4 the findings from the TD group are compared to a group of children with ASD. These results are independent of the amount of artifact in the recording. Bar graphs in Figure 2.4, 2.5, and 2.6 represent the difference in mean power such that positive and negative values represent higher and lower means for the artifact-contaminated segments compared to the means of the artifact-free segments, respectively. Given the large number of comparisons (2 Power Types * 4 Frequency Bands * 9 ROIs * 3 Artifact Types = 216 Comparisons), we have limited the narrative of the results to the most clinically meaningful or relevant trends within the corrected significant results. For completeness and for future reference, we do provide a list of all mean power values and significance values in Table 2.4.

2.7.1 Blinks - Figure 2.5

Mean absolute and relative power was significantly different between blink segments and artifact-free data in all frequency bands. In the theta band, for both absolute and relative power, blink segments had significantly higher power than artifact-free segments, with the most significant differences in frontal regions. In the alpha band, the difference in power varied based on both region and power type. Specifically, the mean relative alpha power in blinks was

significantly lower than artifact-free segments across all ROIs, with the mean absolute alpha power in blinks higher in frontal ROIs and lower in central ROIs. Beta power seemed least affected by blinks, particularly in absolute power, although some differences were evidenced in frontal relative beta power between blinks and artifact-free segments. Finally, and somewhat surprisingly, in the gamma band, blinks did significantly differ from artifact-free segments. They demonstrated higher mean absolute gamma and lower mean relative gamma power than artifact-free segments. These differences were most prominent in the midline regions.

2.7.2 Saccades - Figure 2.6

The mean power differences between saccades and artifact-free segments followed the same general pattern as that of blink segments, with two main distinctions: (1) the magnitude of mean power difference was smaller between saccades and artifact-free segments and (2) significant differences were found in fewer ROIs, particularly central and posterior ROIs. In the theta band, the mean absolute and relative power estimates were higher in saccades than in artifact-free segments. The largest differences in absolute power occurred across frontal regions, but interestingly, relative theta power in the same areas showed no significant differences. In the alpha and beta band, the differences between saccade segments and artifact-free segments mirrored those of blinks. Finally, we found significant differences in mean relative gamma power only in frontal ROI's for saccades compared to artifact-free segments. The mean absolute gamma power, on the other hand, was significantly greater in saccade segments for all midline and central ROIs.

2.7.3 EMG - Figure 2.7

As expected, EMG segments had the highest amount of high frequency power, but they showed significantly different power estimations in all frequency bands compared to artifact-free segments. In the theta band, EMG segments had higher mean absolute power than artifact-free

segments in all ROI's except for midline-central, and had higher mean relative power in the posterior regions. In the alpha band, mean relative power in EMG segments was lower in all regions, while the mean absolute power was unaffected. In the beta band, EMG segments had higher mean absolute and relative power than artifact-free segments in all lateral regions, with some smaller differences seen in the midline ROIs. Finally, in the gamma range, EMG segments showed significantly higher mean absolute and relative power than artifact-free segments in all regions, most prominently in the lateral regions.

2.7.4 Artifacts in ASD vs. TD

The mean number and percent of segments categorized as artifact-free, blink, saccade, or EMG were not significantly different between the ASD and TD groups. Segments categorized as "other" did significantly differ, with the ASD group having on average 11% (approximately 20 segments) more than the TD group ($p < .001$). The total number and percent of artifact-contaminated segments (i.e. the sum of the number of segments in the blink, saccade, EMG, and other categories) was not different between groups. Table 2.2 provides the mean, standard deviation and range in number of segments by category for each group. Figure 2.4 illustrates the same information and provides the average percentages for each category. The effect each type of artifact had on power measurements did not significantly differ in the ASD and TD groups for any power type, band or ROI.

2.8 Discussion

In QEEG studies of young children or developmental populations, participants are often excluded from analysis due to an insufficient amount of artifact-free data. While some studies

have suggested that artifacts, such as blinks, may be included in the analyses with the assumption that they do not affect particular types of power estimations or power bands (Grasser et al., 1985; Hagemann and Naumann, 2001; Iacono and Lykken, 1981), there have been no studies that have directly investigated the potential effect of artifacts on EEG power analysis in young children. The present study was motivated by the goal of characterizing and quantifying the potential effect of artifacts, namely blinks, saccades and EMG, on power estimations in young children, when data quantity does not allow for the use of ICA and other blind source separation (BSS) techniques. In order to address this goal, we used a modeling approach that allowed us to compare equal units of artifacts with artifact-free data in order to understand differences in power that are independent of the amount of data available. By calculating the difference in mean power, we could then consider whether the inclusion of the artifact within the data could affect the power calculation. In other words, a significant difference in mean power in a specific band between an artifact and artifact-free data would suggest that the addition of that artifact to the artifact-free data would affect the calculation of power. The extent of the effect would depend on the total amount of data gathered and the amount of artifact present.

In this study we have demonstrated that in young children, eye blinks, saccades, and EMG contain oscillations of all frequencies and, therefore, could affect the calculation of mean power of both high and low frequency bands, but that the nature and direction of the differences depends on power type, region, and frequency band of interest. Therefore, data processing and cleaning needs to be sensitive to the oscillations of interest for a given analysis, with the most conservative approach being the removal of all EMG and ocular artifact from data. Unfortunately, such an approach leads us to the problem of excluding participants who provide insufficient clean data. The two most robust findings in our study are the following: (1) First, eye movements have

significantly higher relative and absolute theta power than artifact-free data. This result is particularly relevant for studies that induce lateral eye movements and blinks, such as a dynamic visual stimulus (bubbles) during resting-state recordings. The inclusion of blinks in these data will likely result in a spurious increase in the estimation of theta power. (2) Second, the high frequency nature of EMG activity results in higher beta and gamma power in EMG segments than in artifact-free segments, with the greatest difference found in lateral regions that are nearest to facial and neck muscles. Notably, given the lack of significant difference in absolute alpha power, we would conclude that the alpha band does not seem to be affected by EMG, suggesting that in experiments where head and neck movements are difficult to avoid, absolute power in the alpha band may be a more stable target variable. While these results may be intuitive, a quantification of these power differences can help justify the inclusion or exclusion of certain artifact segments in data processing.

Relative vs. Absolute Power

There is tremendous variability in the literature regarding the choice of power type, with studies targeting absolute (e.g. Tierney et al., 2012) or relative power (e.g. Marshall et al., 2002), or both (e.g. Barry et al., 2010), sometimes without an explicit reason provided for the choice. Justifications in favor of relative power include more robust test-retest reliability and less vulnerability to differences in skull thickness which, in turn, may facilitate the analysis of individual differences in early development (Benninger et al., 1984; John, 1980; Nunez and Shrinivasan, 2006). Absolute power, on the other hand, can be easier to interpret since it reflects the actual power value for one given band, without dependence on power in other ranges (Pizzagalli, 2007). Sometimes, the choice of power type is contingent upon methods used in prior studies, particularly when there is a goal is replication or direct comparison of results.

A direct comparison of the extent of artifact effects on absolute vs. relative power (i.e. which is more susceptible to artifacts) is beyond the scope of this work. However, if inclusion of artifact contaminated data in analysis is unavoidable, we support the notion that absolute power is a more intuitive measure and may be less prone to erroneous conclusions, such as false positives, false negatives, or null findings. This is demonstrated through the hypothetical data provided in Table 2.5, and similarly demonstrated through our results for blink artifacts in the alpha and theta bands.

Using hypothetical data, Table 2.5 illustrates three scenarios of how artifact contaminated data may have higher absolute power in separate bands (i.e. each band will appear to have greater absolute power), but the relative power for each band may higher or lower (i.e. bands may appear to have greater or less power). In each of the scenarios, absolute theta and alpha power are higher than in the artifact-free data (scenario 0). Relative power however, may appear higher for both theta and alpha bands (scenario 1); higher for theta, but lower for alpha (scenario 2); or lower for theta, and higher for alpha (scenario 3). This is because relative power reflects the absolute power in one frequency band in relation to the absolute power in all other bands. Even if the absolute power is higher in two bands for artifact contaminated data, the direction of change (i.e. higher or lower) in relative power is unknown. Additionally, note that power band ratios (e.g. theta/alpha) are equivalent for absolute and relative power. This is easily explained by considering how relative power is calculated because the denominators used in relative power calculations cancel out in a ratio of relative powers. In other words, the ratio of two bands in absolute (μV^2) or relative (%) power have no units.

The example given by this hypothetical data is similar to our findings for mean power in Blink segments. Blink segments have higher absolute power in frontal regions for both theta and

alpha bands; however, the increase in the absolute power for the theta band is relatively greater than the increase in the alpha band, thus, the relative alpha power is decreased. The important distinction is that power in the alpha band is not lower in the presence of blinks, it simply did not increase as much relative to power in other frequency bands, primarily the theta band. This is an important distinction that is scarcely discussed in the literature. A summary of our recommendations for selection of power type and frequency bands is provided in Table 2.6.

Regional effects

Our data also show that artifacts might lead to increased or decreased mean power depending on the scalp region. These differences reflect the regional differences in the presence of artifacts such as eye movements and EMG. For instance, an eye blink creates a large amplitude, slow frequency (typically < 5 Hz) deflection in the EEG signal that is most prominent in frontal ROIs (Iacono and Lykken, 1981). Thus, absolute power in the slow theta band is expected to increase especially in frontal ROIs. Even when the mean power measurements in all regions trend in the same direction, the extent to which the regions are affected may not be the same. Such a phenomenon is evidenced in our data by greater differences between EMG and artifact-free data in mean gamma power in lateral ROIs compared to midline ROIs.

Artifacts in ASD vs. TD

The fact that there were no group differences in the effect on power measures for each type of artifact strengthens the confidence in the results from the TD group. Furthermore, as mentioned in the methods section, there is no reason to assume that an electrical signal produced by a physiologic artifact would be different in a neurodevelopmental disorder, such as ASD. This result however, should not be applied to disorders with known anatomic abnormalities such as tuberous

sclerosis, TSC, where the presence and location of tubers in the brain may alter the propagation of both the neural and myogenic signals.

The lack of significant differences in the overall quantity of artifacts, or by type of artifact, between the two groups is similarly encouraging. However, there was a significant difference in the number of segments categorized as "other." After segments were categorized, re-viewing the EEG time-locked video of the child during the recording suggested that "other" segments were often due to: 1) gross movements, such as a child standing up or turning his or her head, or 2) a child touching or pulling the EEG net. This was true for children in both groups, but because there were significantly more "other" segments in the ASD group, these two behaviors may be more frequent in children with ASD or other developmental disorders. It should be noted that this finding may partially be due to segments in the "other" category occasionally containing a combination of artifact types, for example a blink and EMG, or a blink followed by a saccade. Support for this is demonstrated by the slightly lower average number of blink, saccade, and EMG segments in the ASD group (see Table 2.2). Even so, this reason does not entirely explain the highly significant difference.

Future directions

In the analysis of resting-state oscillations, artifacts may, in fact, serve as a proxy for the child's emotional or cognitive state, regardless of whether a child has a developmental disorder. In a recent behavioral study, Oh et al. (2012) found that the spontaneous eye blink rate increased during an attentional task (the Stroop) compared to a resting period, suggesting that blinks may be a proxy for heightened attention or cognitive effort. Whitman et al. investigated the effect of EMG on high frequency oscillations in adults and found that cognitive tasks were associated with greater EMG activity, which, in turn, could confound the calculation of gamma power. We would propose

that, in children, particularly those with atypical development, there can be tremendous variability in emotional and cognitive states even during "resting-state" recordings, with some children requiring additional cognitive control to remain compliant during testing. Such effort or vigilance may theoretically be reflected in their power estimations, such as with higher frontal theta power, but also may be reflected in a higher blink frequency or greater EMG activity. As we continue to expand our interpretation of resting-state oscillations as biomarkers of specific clinical profiles, we may consider artifacts as a clue to the etiology of the spectral power characterizing subgroups or individuals, and we can quantify their presence before discarding them from data processing.

Conclusion

The use of QEEG as a biomarker of typical and atypical development holds promise as a tool to better define more subtle differences between individuals and subgroups within clinical populations, where behavioral measures may not be able to capture clinical heterogeneity. However, only through rigorous and consistent methods for data processing and artifact removal can we truly trust the data at the individual level.

In this chapter we have provided considerable detail about our data collection, preprocessing, artifact identification (without the use of traditional methods such as ICA), and data analysis, in part to reinforce the need for detailed methodological descriptions that will facilitate common practices across study sites and clinical populations. We highlight the need for transparency regarding the choice of relative or absolute power, regions of interest, and frequency band, as each of these variables are differentially vulnerable to artifacts and their interpretation, therefore, depends on the methods used to identify and remove artifacts.

2.9 Tables

Table 2.1: Descriptive and behavioral scores for all enrolled subjects in the ASD and TD groups. Reported values are the group means ± standard deviations, and the group range.

Measure	**ASD** (*n*=67)	**TD** (*n*=47)
Age in months	50.7 ± 13.5, (26.5 – 73.6)	50.3 ± 15.1, (24.4 – 75.2)
Boys : Girls*	46 : 21	26 : 21
IQ**	76.4 ±25.8, (45 – 136)	119.3 ± 14.3, (93 – 153)
Verbal IQ (VIQ)**	79.9 ± 23.9, (55 – 136)	119.1 ± 14.3, (96 – 148)
Non-verbal IQ (NVIQ)**	80.7 ± 24.9, (45 – 131)	111.5 ± 13.3, (88 – 149)
Receptive language (RL)**	77.7 ± 23.9, (50 – 139)	115.5 ± 15.7, (85 – 160)
Expressive language (EL)**	79.2 ± 24.7, (50 – 144)	119.4 ± 13.4, (94 – 152)

*p < .05, ** p << .01

Table 2.2: Number of segments by category. Values reported for the ASD and TD columns represent group means ± standard deviations, with the range in parentheses. Groups only significantly differed in segments categorized as "Other" ($p < 0.001$). The last column is the total number of segments per category (percent of total in parentheses. Of note, the relatively high number of saccades is due to bouncing of bubbles in the video shown during EEG acquisition.

Category	**ASD** (*n*=54)		**TD** (*n*=42)		**Total** (%)
Artifact-Free	63.3 ± 25.6	(23 – 158)	73.9 ± 27.2	(27 – 155)	2269 (51.0)
Blink	14.5 ± 13.3	(1 – 65)	15.6 ± 13.7	(0 – 84)	353 (7.9)
Saccade	19.2 ± 14.2	(0 – 77)	21.1 ± 16.5	(2 – 81)	557 (12.5)
EMG	17.3 ± 17.4	(0 – 72)	22.5 ± 25.6	(0 – 152)	735 (16.5)
Other*	46.0 ± 31.2	(1 – 144)	25.6 ± 22.3	(0 – 87)	534 (12.0)
Total	161.5 ± 48.2	(87 – 290)	158.7 ± 48.5	(115 – 315)	4448 (100)

* $p < .001$

Table 2.3: Number of regions of interest removed by group, due to constant EMG

Missing by ROI	**ASD**	**TD**
Left frontal	8	5
Right frontal	6	1
Left posterior	0	0
Right posterior	2	0

Table 2.4: Mean of log transformed power estimates for segments of EEG data from the Artifact-Free, Blink, Saccade, and EMG categories. Values are given for absolute (uV2) and relative (%) power in the theta (4-7 Hz), alpha (8-12 Hz), beta (13-30 Hz), and gamma (35-45 Hz) frequency bands for each of the 9 ROIs investigated (see figure 1). Bold values for the Blink, Saccade, and EMG categories indicate significant differences in mean power from the Artifact-Free category. Figures 2.4 – 2.6 display graphical representations of these power differences. All significant differences are corrected for multiple comparisons.

			Theta			Alpha			Beta			Gamma		
			Left	Midline	Right	Left	Midline	Right	Left	Midline	Right	Left	Midline	Right
Artifact-Free	Absolute (uV^2)	Frontal	2.02	2.22	2.00	1.04	1.07	1.00	-0.44	-0.83	-0.54	-1.74	-2.39	-1.88
		Central	1.83	1.80	1.73	1.06	0.92	1.02	-0.86	-1.39	-0.89	-2.49	-3.05	-2.47
		Posterior	2.08	2.14	1.99	1.20	1.14	1.12	0.76	0.95	0.79	2.32	2.52	2.35
	Relative (%)	Frontal	3.40	3.54	3.42	2.64	2.62	2.64	2.44	1.99	2.38	0.66	-0.06	0.54
		Central	3.41	3.52	3.43	2.86	2.87	2.94	2.22	1.83	2.32	0.10	-0.32	0.25
		Posterior	3.40	3.47	3.44	2.74	2.69	2.79	2.06	1.88	2.16	0.01	0.18	0.10
Blinks	Absolute (uV^2)	Frontal	2.53****	3.00****	2.50****	1.11	1.29****	1.09**	-0.47	-0.77**	-0.59*	-1.70	-2.27**	-1.88
		Central	1.95***	1.90**	1.87***	0.94***	0.83**	0.90***	-0.88**	-1.40**	-0.93	-2.43	-2.97*	-2.39*
		Posterior	2.28****	2.45****	2.18****	1.07***	1.12	1.06	0.74	-0.89*	0.81	-2.24*	-2.32****	2.29
	Relative (%)	Frontal	3.51****	3.62****	3.49****	2.30****	2.13***	2.31****	2.01****	1.35****	1.91****	0.28***	-0.65***	0.13***
		Central	3.46**	3.54	3.49**	2.67****	2.69****	2.75****	2.13	1.75	2.20****	0.09	-0.32	0.24
		Posterior	3.44	3.53**	3.46	2.46****	2.42****	2.57****	1.93****	1.69****	1.98****	0.06	0.23	0.00**
Saccades	Absolute (uV^2)	Frontal	2.26****	2.47****	2.26****	1.06	1.13	1.02	-0.45	-0.76***	-0.53	-1.78	-2.31**	-1.94
		Central	1.89	1.87*	1.84****	0.99**	0.87	0.93**	-0.87	-1.34*	-0.89	-2.42*	-2.96**	-2.36***
		Posterior	2.15*	2.26****	2.01	1.09****	1.06**	1.00****	-0.76	-0.92	-0.82	-2.32	-2.46*	-2.37
	Relative (%)	Frontal	3.43	3.57	3.44	2.45****	2.45****	2.42****	2.22****	1.85****	2.15****	0.39****	-0.20***	0.25****
		Central	3.45*	3.55	3.46*	2.78**	2.78**	2.77****	2.20	1.84	2.23***	0.15	-0.27	0.27
		Posterior	3.44**	3.55****	3.46	2.61****	2.58****	2.67****	2.04	1.88	2.13	-0.02	-0.15	0.09
EMG	Absolute (uV^2)	Frontal	2.12****	2.36****	2.13****	1.08	1.05	1.06*	-0.03****	-0.75****	-0.14****	-0.77****	-2.00****	-0.92****
		Central	1.98****	1.78	1.87****	1.07	0.79****	1.02	-0.56****	-1.40	-0.56****	-1.65****	-2.84****	-1.63****
		Posterior	2.25****	2.29****	2.11****	1.16	1.12	1.12	-0.54****	-0.84****	-0.56****	-1.65****	-2.10****	-1.67****
	Relative (%)	Frontal	3.26****	3.53	3.31****	2.44****	2.45****	2.46****	2.62****	1.93**	2.54****	1.38****	0.18***	1.27****
		Central	3.32****	3.53	3.35****	2.64****	2.75****	2.72****	2.29**	1.85	2.42****	0.70****	-0.08***	0.86****
		Posterior	3.38	3.51*	3.40**	2.52****	2.56****	2.63****	2.10	1.88	2.23**	0.49****	0.13****	0.63****

$^{*}p < .05$, $^{**}p < .01$, $^{***}p < .001$, $^{****}p < .0001$

Table 2.5: Demonstration of differential artifact effects on absolute versus relative power

Scenario	% Increase in Power from Artifact-Free	Power Type	Theta	Alpha	Beta	Total Power	Theta/Alpha Ratio
0	None (Artifact-Free)	Absolute	70	25	5	100	2.8
		Relative	70.0%	25.0%	5.0%	100%	2.8
1	20% theta & alpha	Absolute	84	30	5	119	2.8
		Relative	70.6% ↑	25.2% ↑	4.2%	100%	2.8
2	25% theta, 20% alpha	Absolute	87.5	30	5	122.5	2.92
		Relative	71.4% ↑	24.5% ↓	4.1%	100%	2.92
3	20% theta, 25% alpha	Absolute	84	31.25	5	120.25	2.69
		Relative	69.9% ↓	26.0% ↑	4.2%	100.0%	2.69

Hypothetical data demonstrating different possible effects of artifacts on absolute and relative power measurements. This table provides one example of how an artifact may have greater absolute power (μV^2) in multiple bands (theta and alpha in scenarios 1-3) compared to artifact-free data (scenario 0), but the effect on relative power (%) measurements is unclear.

Table 2.6: General recommendations for selectionof power type and frequency band.

- Whenever possible, authors should report findings for both absolute and relative power. If discrepancies between the two power types are observed, possible reasons and implications should be discussed.
- Using careful manual artifact detection methods detailed in this manuscript, it is possible to quantify individual artifact types (blinks, saccades, and EMG) and then to separate them from clean, artifact free, segments of data. The separation of artifacts allows for the flexibility of either including or excluding them based on the type of analyses being performed.
- If there is a risk of data contamination due to blinks or saccades, investigations of absolute and relative power in theta and alpha bands, and relative power for the beta and gamma bands, in frontal regions should be avoided (Figure 2 & 3). Posterior gamma power is least likely to be affected by eye movement artifact.
- If there is a risk of data contamination due to EMG, investigations of absolute and relative power in absolute and relative beta and gamma bands, in all regions should be avoided (Figure 4). Posterior alpha power is least likely to be affected by EMG artifact.
- If the results for only one power type can be reported (e.g. due to space limitations) and multiple frequency bands are compared, absolute power is preferred because the potential effects of artifacts on relative power for each frequency band are more unpredictable.
- Artifacts themselves may provide insight into the state of a child which can, in turn, inform individual differences in power.

2.10 Figures

Figure 2.1: Range in standard scores for cognitive assessments for the ASD and TD groups.

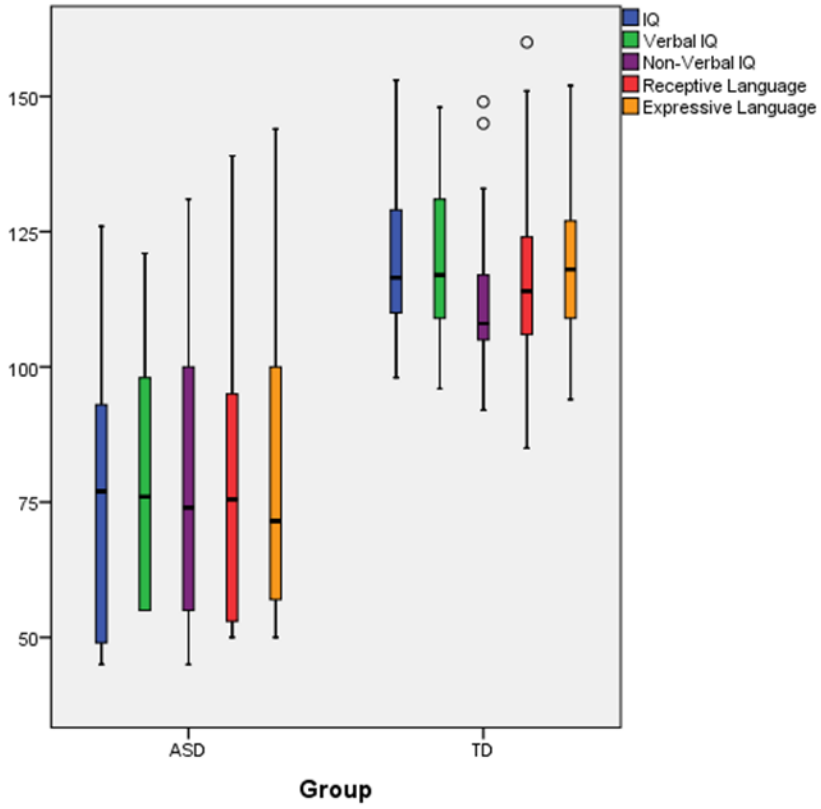

Figure 2.2: Nine regions-of-interest (ROI) were selected to provide maximal spatial coverage of the left (red), midline (green), and right (blue) portions of frontal (diamonds), central (stars), and posterior (squares) scalp regions. All ROIs contain 4 electrodes, except for the midline-central ROI which contains 5 electrodes. The approximate 10-20 system electrode equivalents and the channel numbers for the regions are: ***F3*** *= 23, 24, 27, 28;* ***Fz*** *= 5, 11, 12, 16;* ***F4*** *= 3, 117, 123, 124;* ***C3*** *= 35, 36, 41, 42;* ***Cz*** *= 7, 31, 80, 106, Ref;* ***C4*** *= 93, 103, 104, 110;* ***P3*** *= 51, 52, 59, 60;* ***Pz*** *= 62, 71, 72, 76; and* ***P4*** *= 85, 91, 92, 97. Channels 125 – 127 (marked with an X) were originally located below or lateral to the eyes, but were removed to make wearing the net more comfortable for children. Interpolated signals were calculated most often for electrodes located along edge of a net.*

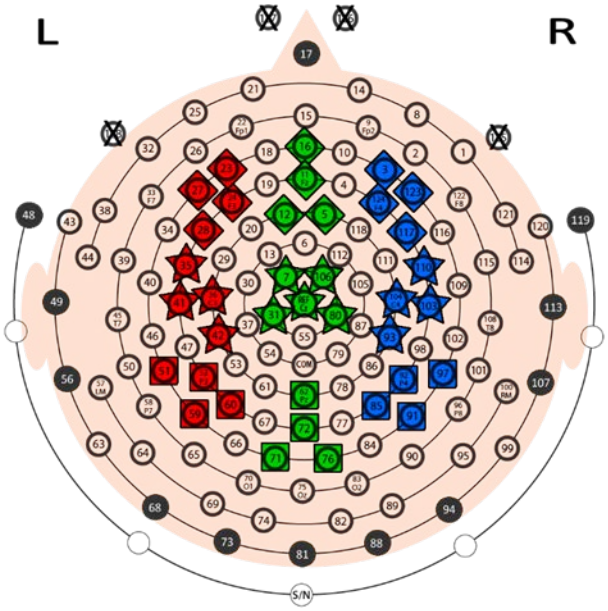

Figure 2.3: Representative examples of a (A) blink, B) saccade, and C) EMG artifact.

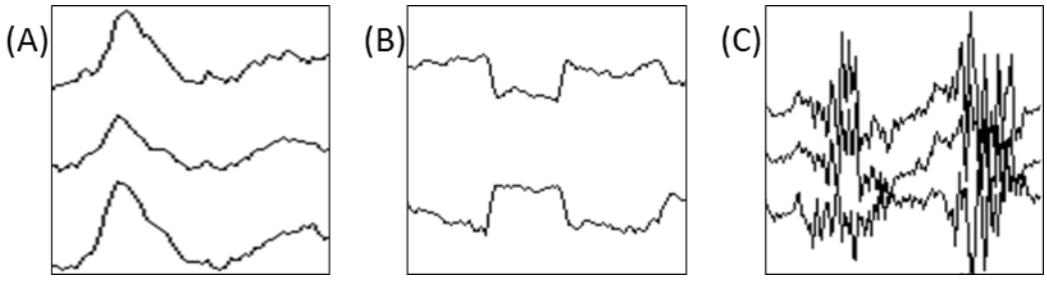

Figure 2.4: Mean and percentages for segments categories for the ASD and TD groups

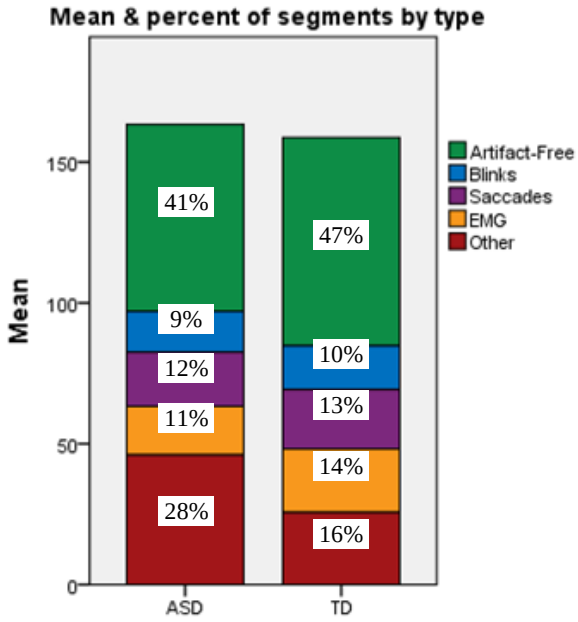

Figure 2.5: Differences in mean power for the Blink and Artifact-Free categories (i.e. $Power_{Blink}$ – $Power_{Artifact\text{-}Free}$). Positive values represent higher power in the Blink category. Figure 2.6 and 2.7 display the same information (i.e. $Power_{Artifact}$ – $Power_{Artifact\text{-}Free}$) for saccade and EMG artifacts, respectively. Power values were log transformed (see Table 2.4) prior to calculation of differences. All significant differences (*) are $p < 0.05$ and corrected for multiple comparisons.

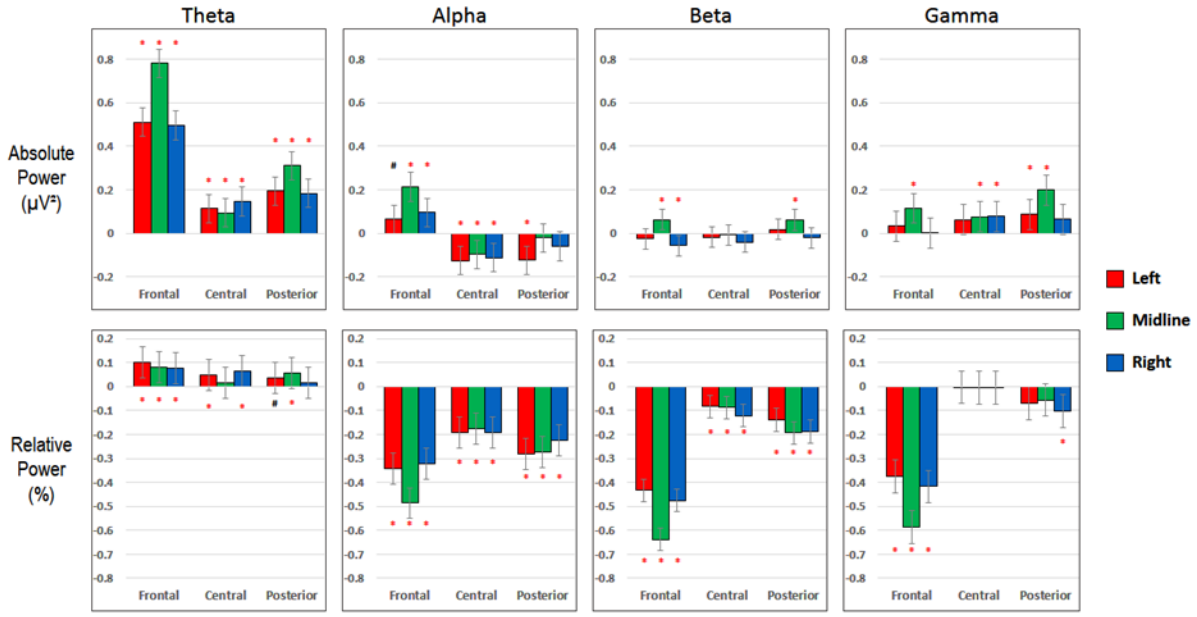

Figure 2.6: Differences in mean power for the Saccade and Artifact-Free categories (i.e. Power$_{Saccade}$ – Power$_{Artifact\text{-}Free}$). See the caption of Figure 2.5 for details.

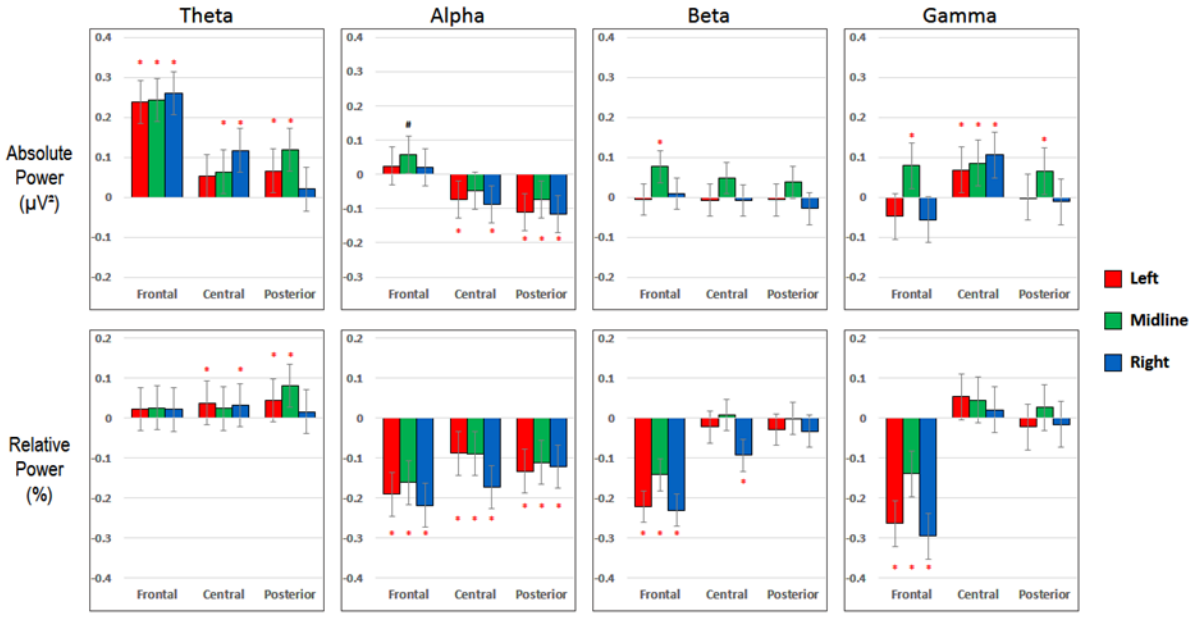

Figure 2.7: Differences in mean power for the EMG and Artifact-Free categories (i.e. $Power_{EMG}$ – $Power_{Artifact\text{-}Free}$). See the caption of Figure 2.5 for details.

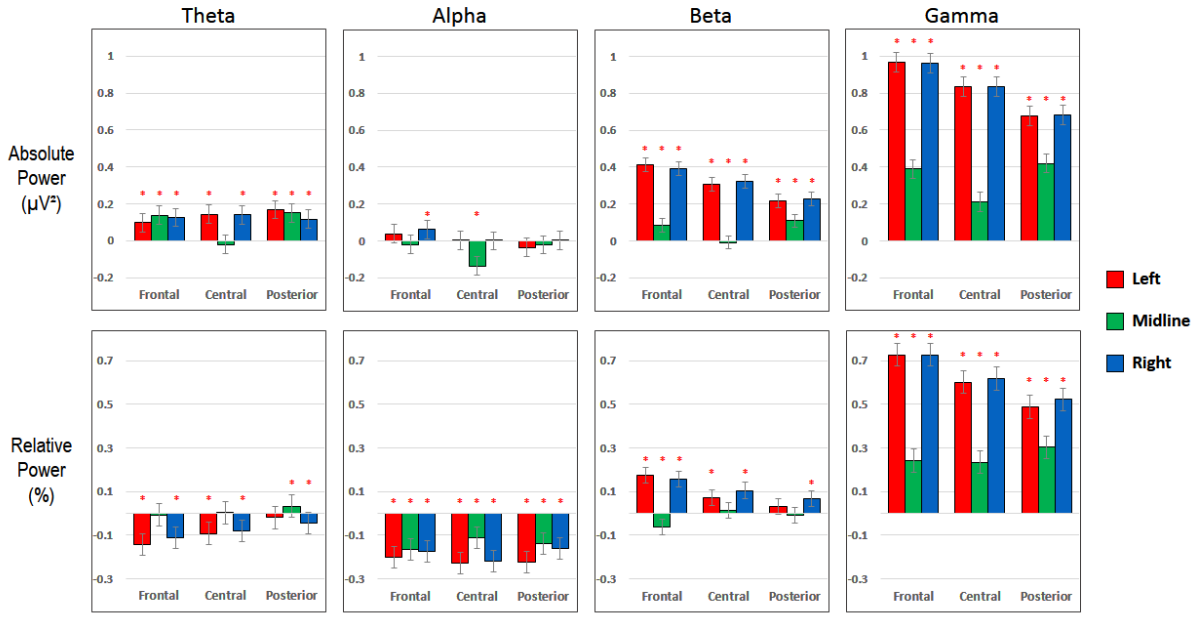

Chapter 3: Modeling ASD Phenotypes & EEG Band Power

3.1 Introduction

The primary aims of this dissertation are 1) to assess the current use of resting-state QEEG band power measures for studying children with ASD, and 2) investigate differences from typically developing controls. The previous chapter addressed this by assessing how artifacts may affect band power measures, and if they could be responsible for any observed group differences. Attention is now turned to how behavioral measures of individuals affect differences in band power between the two groups. Standardized assessments of behavior are a means of quantifying individual differences in phenotypes and cognitive abilities. Measures of QEEG band power also quantify aspects of phenotypic differences, but from a physiologic perspective. With the broad spectrum of phenotypes observed across children with ASD, it is likely that different phenotypes and behaviors will differentially affect band power. Nearly all studies of band power in individuals with ASD limit their analysis strictly to band power differences, ignoring the diversity across ASD. Without accounting for phenotypic variability, band power differences could erroneously be attributed to the disorder, when in reality should be attributed to a behavior commonly associated with the disorder, such as language impairments.

Failing to account for the variability in ASD is likely to result in different findings across research groups. Recent literature reviews highlight this problem of conflicting results in ASD research on resting-state QEEG (Billeci et al., 2013; Cantor & Chabot, 2009; Wang et al., 2013).

As the reviews discuss, identifying a pattern of QEEG differences that are unique to ASD is hampered by relatively few studies, many of which differ drastically in ASD population studied (e.g. high functioning adults vs. low function children), data processing strategies, and the QEEG measures investigated (e.g. type of power calculation, frequency bands, regions of interest, etc.). Despite these differences, the aim of these studies were the same. Specifically, they sought to determine if measures of QEEG band power are different in individuals with and without ASD, i.e. a main effect of ASD. If consistent differences were discovered, this would indeed be a very important finding; however, no single pattern of differences has been identified. This may be due to the large degree of heterogeneity observed across both individuals with ASD, and across experimental designs. One strategy for dealing with the heterogeneity is to include phenotypic measures in statistical models. Thus, the current chapter investigates the effect of including behavioral assessments in statistical analysis of band power measures in ASD, and if differences can be attributed to the behavior, the disorder, or even both.

Therefore, we first determine that individual phenotypic measures are significant predictors of band power measures in children with ASD and should be included in statistical analyses. We then apply this principle to investigation of group differences across frequency bands.

Incorporating phenotype in analyses

Traditional statistical methods used to investigate band power are not well suited for incorporating phenotype data into the analysis. Most QEEG studies rely on repeated measure ANOVAs (analysis of variance), one of several statistical tests within general linear models (GLM), to test for significant differences. A major assumption of many statistical tests is independence between variables. The band power measures from QEEG typically violate this

assumption because of the high correlation between the multiple measures from individual subjects, for example across multiple regions of interest (ROIs). Repeated measure ANOVAs, however, specifically test the differences in means between related dependent variables, which make them appropriate. In addition to being relatively straight forward to implement and interpret results, extensions of this method offer other advantages. In an orthogonal two-way repeated measure ANOVAs, two sets of independent variables can be included, for example separate ROIs for each hemisphere.

A repeated measure ANOVA also makes assumptions, which can limit its usefulness - for example, it cannot handle unbalanced data (i.e. missing or incomplete data). In the present study, this would force many subjects to be removed from analysis for both the ASD (n = 13) and TD (n = 5) groups. These subjects needed to be excluded from analysis in select ROIs because it contained low amplitude, constant muscle. From a statistical standpoint, this means many children from both groups have incomplete data (see supplementary info). For the ASD group in particular, measures on cognitive assessments for some of the children with incomplete data suggested they were quite cognitively impaired. These children represent an important cohort within ASD. Rather than remove these children from analysis and lose otherwise clean data, multilevel modeling was used for tests of significance.

Multilevel modeling (MLM), also referred to as hierarchical linear modeling, is a powerful, generalized form of GLMs. The flexibility of MLMs enable it to account for missing data and to overcome some of the other assumptions made by various GLM tests, such as independence between predictors and homogeneity of regression slopes (Field, 2009). Where the GLM relies on ordinary least squares (OLS) to determine the fit of model parameters, MLM can use link functions

to overcome assumptions violated in GLMs (e.g. non-normal data), and iterative methods (e.g. maximum-likelihood estimation) to determine the fit of a model.

Because it allows the inclusion of both fixed (e.g. main effects) and random effects (e.g. subject specific differences), MLM is able to address questions not suitable for repeated measure ANOVAs. A multilevel model approach that examines band power differences between children with ASD and TD controls, provides a unique strategy to account for the individual, subject specific differences which may have contributed to the mixed findings reported in research literature. By including sources of variability in analyses, MLM can directly test if observed differences are due to the disorder or phenotypes observed in the disorder.

The models used in this chapter were built through a recommended series of steps (adapted from Peugh, 2010):

1. Clarify the research question
2. Choose the parameter estimation method
3. Assess the need for MLM
4. Build the level-1 model
5. Build the level-2 model
6. Determine multilevel effect sizes
7. Test competing multilevel models

We begin by comparing four different models built using this approach and describe the full model used for the remainder of the analyses. Next we apply the full model to all frequency bands, and determine which model parameters were significant predictors of band power measures.

3.2 Methods

3.2.1 Participants and Data

The data for the current analysis were gathered from the same population used in the previous chapter. See section 2.2 above for details of data acquisition and processing methods. Only children who contributed a minimum of 30 seconds of clean, artifact-free data were included in the current analysis (N = 96; ASD: n = 54; TD: n = 42). Measures for phenotype were based on language and cognitive assessments reported in the previous chapter (see Table 2.1).

The previous chapter noted that a band's power is influenced by other bands when relative power calculations are used. As such, this chapter focuses on calculations of absolute power only. Consistent with our recommendations in the previous chapter however, the results for relative band power are provided in Table 3.4 and Table 3.5 for reference, with notable differences mentioned in the discussion section. The frequency range for the bands investigated were: delta (1-3 Hz), theta (4-7 Hz), alpha (8-12 Hz), beta (13-30 Hz), and gamma (35-45 Hz) bands. Power measurements were taken from 4 regions of interest (ROI): left-frontal, right-frontal, left-posterior, and right posterior (Figure 3.1). Relative to the previous chapter, fewer ROIs were investigated, but each included additional electrodes, thus covering a larger portion of the scalp. We reduced the number of ROIs analyzd in order to decrease the number of parameters used in statistical comparisons, while maintaining a maximal spatial sampling of the neural activity across the scalp.

3.2.2 Statistical Models & Analysis

Statistical modeling and analysis were performed in SPSS (IBM SPSS Statistics for Windows, Armonk, NY). Model parameter estimates were calculated using the MIXED procedure,

with bootstrapping (1000 samples with replacement per model) to improve the accuracy of confidence intervals and standard errors.

The importance of including phenotype data (e.g. age, language function, etc.) is demonstrated through a statistical comparison of four progressive models of absolute frontal theta power (Table 3.1). Two models can be compared when all parameters from one of the models are nested (i.e. a subset) within the larger model. The difference between each model's deviance (i.e. – 2 Log Likelihood) and degrees of freedom can then be used in chi squared (χ^2) tests to determine if the larger model is a significantly better fit of the data. The results provided in Table 3.1 list χ^2 tests for (a) Model 1 compared directly to each of the larger models, and (b) each model to the model nested immediately before it, meaning Model 2 vs. 1, Model 3 vs. 2, and Model 4 vs. 3. Model 3.

Level-1: $$Y_{ij} = \beta_{0j} + \beta_{1j} HEMI_{ij} + r_{ij}$$

Level-2: $$\beta_{0j} = \gamma_{00} + \gamma_{01} GROUP_j + \gamma_{02} AGE_j + \gamma_{03} LANG_j + u_{0j}$$

Level-2: $$\beta_{1j} = \gamma_{10} HEMI_{ij} + \gamma_{11} HEMI_{ij} * GROUP_j$$

Full Model: $$Y_{ij} = \gamma_{00} + \gamma_{01} GROUP_j + \gamma_{10} HEMI_{ij} + (\gamma_{11} HEMI_{ij} * GROUP_j) + \gamma_{02} AGE_j + \gamma_{03} LANG_j + u_{0j} + r_{ij}$$

Each model is composed of a response variable and predictor variables at two levels, within-subject and between-subject. The response variable (Y_{ij}) is the measured band power within a hemisphere i (level-1; left = 0, right =1) for each child j (level-2). To account for the high

correlation between power measures from separate hemispheres within the same subject, a random effect (u_{0j}) was included, which allows intercepts to vary across subjects. The remainder of the parameters assessed are fixed effects, and include:

- GROUP (γ_{01}): dichotomous variable; indicates the group assignment (ASD = 0, TD = 1).
- HEMI (γ_{10}): dichotomous variable; indicates the hemisphere of the power measurement (0 = left, 1 = right). Note, a parameter indicating if a measured power corresponded to a frontal versus posterior ROI was not needed because each were analyzed in separate models.
- GROUP*HEMI (γ_{11}): interaction term; used assess group differences in power asymmetry.
- AGE (γ_{02}): continuous variable; represents a child's age in months at the time of the recording. Preliminary analysis of correlation indicated that a child's age had a strong negative correlation with absolute power across all bands and for both groups. Even though age did not correlate with relative power, age is still included in the models for relative power analysis to prevent confusion.
- LANG (γ_{03}): continuous variable; measure of a child's expressive language ability based on standardized scores from behavioral assessments.
- IQ (γ_{04}): continuous variable; standardized scores from IQ assessments.

Data from frontal and posterior ROIs were analyzed in separate models since a comparison of power between these regions was not of interest. Although it is possible to include frontal and posterior ROIs in the same model, the correlation between measures obtained from single subjects is complex. For example, power measured in the left-frontal ROI typically correlates more with

its contralateral equivalent (i.e. the right-frontal ROI) than with its ipsilateral (i.e. the left-posterior ROI). Without including a covariance structure to account for this relationship, statistical assumptions will be violated and the residuals of the model are likely to correlate.

After assessing the models, the full model used throughout the remainder of the chapter is Model 3. Results from the full model are reported for 20 separate analyses, corresponding to each of the 5 frequency bands, 2 power types, and 2 sagittal regions (frontal and posterior). Each model's threshold for significance was adjusted for multiple testing by controlling for the false discovery rate (FDR).

To facilitate comparisons across frequency bands, power measures were mean centered within each ROI and regions. For example, measures of absolute theta power in the left-frontal ROI from all subjects were averaged, and this value was then subtracted from each individual measure of the theta power in the left-frontal ROI ($X_{left\ frontal,j} - \bar{X}$). It is important to note that this technique only adjusts estimate of the intercept (γ_{00}), essentially scaling it and the standard error. The estimate and significance for other parameters is unaffected.

3.3 Results

Model Assessments

Using absolute theta power from frontal regions as a demonstration, Table 3.2 lists the estimated parameter values for each of the four tested models. In the simplest model (Eq 1), none of the fixed effect parameters significantly predicted absolute theta power. In the second model (Eq 2), AGE was a significant predictor ($F(1, 8.6)$, $p << .001$), and compared to the first model,

AGE also significantly improved the model's fit ($\chi^2(1) = 8.2$, $p < 0.005$). Including a measure of language function, LANG, in the third model (Eq 3) resulted in three of the fixed effects significantly predicting absolute frontal theta power: GROUP ($\gamma_{01} = -0.18$, $F(1, 3.8)$, $p < .001$), AGE ($\gamma_{02} = -0.007$, $F(1, 8.6)$, $p < .001$), and LANG ($\gamma_{03} = -0.003$, $F(1, 3.0)$, $p < .005$). However, IQ was not a significant predictor when included in a model already containing AGE and LANG ($\gamma_{04} = 0.002$, $F(1, 0.4)$, ns), as seen in the last model (Eq 4).

The difference in deviance statistics between the simplest model (Eq 1) and subsequent models (Eq 2 – 4) demonstrates that these models were significantly better, meaning they provided a better fit of the observed theta power. (Eq 1 vs. 2: $\chi^2(1) = 8.2$; Eq 1 vs 3: $\chi^2(2) = 11.2$; Eq 1 vs. 4: $\chi^2(3) = 11.5$, all $p < 0.005$). However, models 3 was only a moderate improvement over model 2 (Eq 2 vs. 3: $\chi^2(1) = 3.0$, $p = .08$), and model 4 was not an improvement over model 3 (Eq 3 vs. 4: $\chi^2(1) = 0.4$, ns).

Including a subject-level intercept, a random effect (τ_{00}), accounted for the collinear relationship between measures taken from the same subject (i.e. left and right ROIs). It was also significant in the full model (Eq 3) for the rest of the frequency bands (Tables 3.3 through 3.6). This parameter was highly significant in all models ($p < .001$), which supports using multilevel modeling as our statistical approach. Calculations of the intraclass correlations (ICC) further support the need for multilevel modeling. Higher ICC values suggest unequal variations in level-1 (within subject) and level-2 units (between subject), and can be accounted for in multilevel modeling. The ICC for the unstructured model demonstrated that level-2 variation (i.e. between-subjects) in band power ranged from 56% to 83%, depending on the frequency band. This suggests there was a large degree of the variation in band power measures across subjects.

Full Model Estimates

Tables 3.3 and 3.4 list the parameter estimates from the full model for absolute band power in frontal and posterior regions, respectively. Estimates for relative power are provided in Tables 3.5 and 3.6 for reference.

Across all bands, the predictors in the model were most significant for the theta band. Specifically, children with ASD had significantly lower absolute theta power than children in the TD group regardless of region (Theta: $GROUP_{Frontal}\ \gamma_{01}$ = -0.18 F(1,~92) = 3.8; $GROUP_{Posterior}\ \gamma_{01}$ = -0.15, F(1,~96) = 2.4). A similar trend was observed for the delta band, but was not significant after adjusting for multiple comparisons (Delta: $GROUP_{Frontal}\ \gamma_{01}$ = -0.12 F(1,~93) = 2.7; $GROUP_{Posterior}\ \gamma_{01}$ = -0.13, F(1,~95) = 2.7). Figure 3.2 illustrates the effect of GROUP by showing that typically developing children are predicted to have higher absolute power in lower frequency bands than children in the ASD group across all scalp regions.

The expressive language measure, LANG, also significantly predicted absolute theta and delta power regardless of scalp region (delta: $LANG_{Frontal}\ \gamma_{03}$ = -0.003 F(1,~93) = 4.1; $LANG_{Posterior}\ \gamma_{03}$ = -0.003 F(1,~96) = 4.4; theta: $LANG_{Frontal}\ \gamma_{03}$ = -0.003 F(1,~92) = 3.0; theta: $LANG_{Posterior}\ \gamma_{03}$ = -0.003 F(1,~96) = 3.8).

The AGE parameter was a highly significant, negative predictor ($p < 0.005$ corrected) of absolute power in frontal and posterior regions for all bands, except for beta power in frontal regions. The negative value of this estimate implies that for every unit increase in age (i.e. 1 month), a child's absolute band power[1] is expected to decrease, on average, by the estimated value for the AGE parameter, respectively for each band. This age related decrease is most important for

[1] N.B. Absolute band power (μV^2) values were natural log transformed [$\log_e (\mu V^2)$]. Therefore the magnitude of an increase or decrease should be back transformed by e^x to get the change in absolute power. For example, a change of .01 for a natural log transformed power value is actually equal to a change by 1.01 μV^2 ($e^{.01} = 1.01$).

measures of absolute power. For relative power, a child's AGE was only a significant predictor of relative band power for posterior theta (γ_{02} = -0.001, F(1,~96) = 1.8), frontal beta (γ_{02} = 0.005 F(1,~92) = 4.7), and posterior beta (γ_{02} = 0.005 F(1,~96) = 6.2) (all $p < .05$ corrected).

The parameters for the main effect of hemispheric source, HEMI, and the interaction of group and hemisphere, GROUP*HEMI, were not significant for any region or band. This means 1) knowing which hemisphere (left or right) a measured power originates from does not help predict the observed power, and 2) children with ASD do not have predictable different power in any specific hemispheric region than typically developing children.

3.4 Discussion

This analyses focused on a model of resting-state band power to determine if having a diagnosis of ASD improved band power estimates when individual characteristics (e.g. age, ROI, etc.) are also included in the model. The results based on the model used here suggest a child's age was the only significant predictor of resting-state band power. Simply having a diagnosis of ASD (i.e. GROUP), without other phenotypic information, was not helpful. This result is not surprising due to the large heterogeneity across individuals with ASD. A more complex model, one which includes additional measures of ASD severity and characteristics, is likely needed. A more accurate model, for example, may include measures of verbal and non-verbal skills, repetitive behaviors, IQ, age, gender, genetic markers, etc. By including additional phenotypic information more complex models have the potential to determine if true group differences exist, but are potentially masked by a large variability in other characteristics (e.g. language ability) or even

their interactions (e.g. ASD and female). Furthermore, by including additional phenotypic parameters in a model of resting-state band power, researchers can determine if group differences are markers of core ASD deficits or rather a reflection of other traits.

Clinical diagnosis has embraced the heterogeneity within ASD, best exemplified by the changes to the diagnostic criteria seen in the most recent The Diagnostic and Statistical Manual of Mental Disorders, Fifth Edition (DSM-5). The previous diagnosis used separate names (e.g. Asperger's disorder, childhood disintegrative disorder, etc.) to subgroup what were believed to be diagnostically distinct types of autism, occasionally referred to as "the autisms." According the American Psychiatric Association (APA), "the revised diagnosis represents a new, more accurate, and medically and scientifically useful way of diagnosing individuals with autism-related disorders (Autism Spectrum Disorder Fact Sheet, APA, 2014)." Other changes to the diagnosis made by the DSM-5 account for the spectrum aspect of ASD by requiring specification of various features of the disorder that are present in the child, for example with or without language impairment. The results, or lack of group differences, reported here support the changed approach to the ASD diagnosis because when the heterogeneity within a diverse group of children is ignored they are treated as a single, homogeneous group then differences from TD children in band power are not observed.

Even though there are a few examples of researchers acknowledging the heterogeneity within ASD by specifically studying subgroups of individuals with ASD (Cantor et al., 1986; Dawson et al., 1995; Sutton et al., 2005), the majority of QEEG studies treat all subjects within the ASD group as a single group distinct from the control group. Combining everyone with ASD into one group relies on a common assumption made by many research studies that the individuals in the experimental group (e.g. drug, treatment, disorder, etc.) are more closely related to each

other than individuals in the control group (e.g. placebo, no treatment, disorder-free, etc.). However, this assumption does not seem appropriate when studying ASD because of the known heterogeneity. Instead, one of the main points of this dissertation is that studies on ASD should focus on closely related subgroups of individuals (e.g. individuals with language impairment but no intellectual impairment – discussed in the next chapter) or specific aspects of the disorder (e.g. repetitive behaviors).

3.5 Tables

Table 3.1: Equations used for multilevel model assessments. Equation 1 is the simplest, nested model; it includes fixed effect parameters for the intercept (γ_{00}), GROUP (γ_{01}), HEMI (γ_{10}), the interaction of GROUP and HEMI (γ_{11}), a random effect that allows the intercept to vary for each subject (u_{0j}), and a term for the residual error (r_{ij}). The response variable, Y_{ij}, represents the observed power measured in the left (i = 0) or right (i = 1) hemisphere of subject = j. Equations 2 through 4 progressively add additional fixed effects for AGE (γ_{02}), LANG (γ_{03}), and IQ (γ_{04}), respectively (bold). Equation 3 is the full model used throughout the rest of this chapter.

Equation	Equation
(1)	$Y_{ij} = \gamma_{00} + \gamma_{01}GROUP_j\gamma_{10}HEMI_{ij} + (\gamma_{11}HEMI_{ij} * GROUP_j) + u_{0j} + r_{ij}$
(2)	$Y_{ij} = \gamma_{00} + \gamma_{01}GROUP_j + \gamma_{10}HEMI_{ij} + (\gamma_{11}HEMI_{ij} * GROUP_j) + \boldsymbol{\gamma_{02}AGE_j} + u_{0j} + r_{ij}$
(3)	$Y_{ij} = \gamma_{00} + \gamma_{01}GROUP_j + \gamma_{10}HEMI_{ij} + (\gamma_{11}HEMI_{ij} * GROUP_j) + \gamma_{02}AGE_j + \boldsymbol{\gamma_{03}LANG_j} + u_{0j} + r_{ij}$
(4)	$Y_{ij} = \gamma_{00} + \gamma_{01}GROUP_j + \gamma_{10}HEMI_{ij} + (\gamma_{11}HEMI_{ij} * GROUP_j) + \gamma_{02}AGE_j + \gamma_{03}LANG_j + \boldsymbol{\gamma_{04}IQ_j} + u_{0j} + r_{ij}$

Table 3.2: Parameter estimates from model building assessment

Parameter	Variable	Model 1		Model 2		Model 3		Model 4	
Model Fit: Deviances									
-2 Log Likelihood (-2LL)		27.6		19.4		16.4		16.0	
Degrees of Freedom (*df*)		6		7		8		9	
$\chi^2_{\text{Deviance from Model 1}}$				**8.2***		**11.2***		**11.5***	
$\chi^2_{\text{Deviance from Preceding Model}}$				**8.2***		3.0†		0.4	
Regression Coefficients: Fixed Effects									
Intercept	γ_{00}	0.040	(0.032)	**0.408****	(0.069)	**0.734****	(0.118)	**0.682****	(0.124)
GROUP	γ_{01}	-0.063	(0.045)	-0.069	(0.043)	**-0.182****	(0.056)	**-0.161***	(0.060)
HEMI	γ_{10}	-0.001	(0.045)	0.000	(0.047)	0.000	(0.045)	0.000	(0.044)
GROUP*HEMI	γ_{11}	0.004	(0.059)	0.003	(0.058)	0.002	(0.059)	0.002	(0.057)
AGE	γ_{02}			**-0.007****	(0.001)	**-0.007****	(0.001)	**-0.007****	(0.001)
LANG	γ_{03}					**-0.003***	(0.001)	**-0.004***	(0.002)
IQ	γ_{04}							0.002	(0.002)
Variance Components: Random Effects									
Residual	σ^2	0.020	(0.003)	0.020	(0.003)	0.020	(0.003)	0.020	(0.713)
Intercept	τ_{00}	**0.101****	(0.011)	**0.091****	(0.010)	**0.088****	(0.010)	**0.088****	(0.001)

Estimates are calculated from absolute theta power measured in left and right frontal ROIs (standard errors in parentheses). χ^2 tests are based on the difference between model deviances (i.e. -2 Log Likelihoods) and each model's degrees of freedom. $\chi^2_{\text{Deviance from Model 1}}$ compares Model 1 directly to each of the other models. $\chi^2_{\text{Deviance from Preceding Model}}$ compares a model to the model in the column to its left, e.g. Model 3 vs. Model 2, and Model 4 vs. Model 3. † $p < 0.1$, * $p < 0.005$, ** $p < .001$

Table 3.3: Parameter estimates for absolute power in frontal regions

Parameter Estimates – Absolute Power – Frontal Regions

Parameter	Variable	Delta		Theta		Alpha		Beta		Gamma	
Regression Coefficients: Fixed Effects											
Intercept	γ_{00}	0.692	(0.117)	0.734	(0.007)	0.478	(0.136)	0.387	(0.16)	0.473	(0.175)
GROUP	γ_{01}	**-0.119**†	(0.058)	**-0.182***	(-0.008)	-0.082	(0.067)	-0.106	(0.072)	0.015	(0.087)
HEMI	γ_{10}	0.013	(0.045)	< 0.000	(-0.002)	-0.007	(0.052)	0.019	(0.055)	0.018	(0.062)
GROUP*HEMI	γ_{11}	-0.010	(0.07)	0.002	(0.003)	0.019	(0.066)	-0.013	(0.071)	0.002	(0.09)
AGE	γ_{02}	**-0.007***	(0.001)	**-0.007***	(< 0.001)	**-0.008***	(0.002)	-0.002	(0.002)	**-0.011***	(0.002)
LANG	γ_{03}	**-0.003***	(0.001)	**-0.003***	(< 0.001)	0.000	(0.001)	-0.002	(0.001)	0.001	(0.001)
Variance Components: Random Effects											
Residual	σ^2	0.029	(0.003)	0.020	(0.003)	0.024	(0.003)	0.026	(0.003)	0.045	(0.005)
Intercept	τ_{00}	**0.062***	(0.008)	**0.088***	(0.01)	**0.185***	(0.016)	**0.180***	(0.021)	**0.179***	(0.018)

Parameter estimates from Model 3, the full model (standard errors in parentheses). * $p < 0.05$ corrected; † $p < 0.05$ uncorrected.

Table 3.4: Parameter estimates for absolute power in posterior regions

Parameter Estimates – Absolute Power – Posterior Regions

Parameter	Variable	Delta		Theta		Alpha		Beta		Gamma	
Regression Coefficients: Fixed Effects											
Intercept	γ_{00}	0.977	(0.135)	1.083	(0.116)	0.679	(0.143)	0.550	(0.137)	0.702	(0.129)
GROUP	γ_{01}	**-0.133†**	(0.069)	**-0.151†**	(0.057)	-0.084	(0.071)	-0.038	(0.061)	0.058	(0.06)
HEMI	γ_{10}	0.016	(0.075)	-0.006	(0.053)	-0.001	(0.042)	0.006	(0.036)	-0.009	(0.043)
GROUP*HEMI	γ_{11}	-0.045	(0.087)	-0.008	(0.061)	-0.002	(0.06)	-0.012	(0.049)	0.003	(0.063)
AGE	γ_{02}	**-0.011***	(0.001)	**-0.013***	(0.001)	**-0.013***	(0.002)	**-0.007***	(0.001)	**-0.014***	(0.001)
LANG	γ_{03}	**-0.003***	(0.001)	**-0.003***	(0.001)	0.001	(0.001)	-0.002	(0.001)	< 0.000	(0.001)
Variance Components: Random Effects											
Residual	σ^2	0.052	(0.005)	0.023	(0.003)	0.023	(0.002)	0.016	(0.002)	0.027	(0.003)
Intercept	τ_{00}	**0.083***	(0.012)	**0.112***	(0.01)	**0.220***	(0.016)	**0.170***	(0.017)	**0.126***	(0.013)

Parameter estimates from Model 3, the full model (standard errors in parentheses). * $p < 0.05$ corrected; † $p < 0.05$ uncorrected.

Table 3.5: Parameter estimates for relative power in frontal regions

Parameter Estimates – Relative Power – Frontal Regions

Parameter	Variable	Delta		Theta		Alpha		Beta		Gamma	
Regression Coefficients: Fixed Effects											
Intercept	γ_{00}	0.056	(0.056)	0.083	(0.04)	-0.188	(0.092)	-0.279	(0.114)	-0.185	(0.162)
GROUP	γ_{01}	0.017	(0.021)	**-0.044***	(0.017)	0.054	(0.044)	0.026	(0.047)	**0.144***	(0.078)
HEMI	γ_{10}	0.009	(0.018)	-0.004	(0.012)	-0.007	(0.028)	0.016	(0.037)	0.016	(0.059)
GROUP*HEMI	γ_{11}	-0.010	(0.026)	-0.002	(0.019)	0.007	(0.036)	-0.021	(0.052)	-0.005	(0.08)
AGE	γ_{02}	< 0.000	(0.001)	< 0.000	(< 0.001)	-0.001	(0.001)	**0.005***	(0.001)	**-0.003†**	(0.002)
LANG	γ_{03}	-0.001	(< 0.001)	< 0.000	(< 0.001)	**0.002***	(0.001)	< 0.000	(0.001)	**0.003***	(0.001)
Variance Components: Random Effects											
Residual	σ^2	0.004	(< 0.001)	0.002	(< 0.001)	0.008	(0.001)	0.015	(0.002)	0.039	(0.004)
Intercept	τ_{00}	**0.022***	(0.003)	**0.009***	(0.001)	**0.062***	(0.005)	**0.089***	(0.009)	**0.164***	(0.016)

Parameter estimates from Model 3, the full model (standard errors in parentheses). * $p < 0.05$ corrected; † $p < 0.05$ uncorrected.

Parameter Estimates – Relative Power – Posterior Regions

Parameter	Variable	Delta		Theta		Alpha		Beta		Gamma	
Regression Coefficients: Fixed Effects											
Intercept	γ_{00}	0.061	(0.059)	0.191	(0.038)	-0.228	(0.1)	-0.351	(0.104)	-0.178	(0.123)
GROUP	γ_{01}	-0.009	(0.026)	**-0.045***	(0.017)	0.026	(0.048)	0.067	(0.041)	**0.161***	(0.061)
HEMI	γ_{10}	0.010	(0.028)	-0.010	(0.009)	-0.008	(0.032)	-0.006	(0.039)	-0.026	(0.054)
GROUP*HEMI	γ_{11}	-0.021	(0.034)	0.013	(0.013)	0.023	(0.046)	0.020	(0.05)	0.043	(0.07)
AGE	γ_{02}	< 0.000	(0.001)	**-0.001***	(< 0.001)	-0.001	(0.001)	**0.005***	(0.001)	**-0.002†**	(0.001)
LANG	γ_{03}	< -0.001	(< 0.001)	**-0.001***	(< 0.001)	**0.003***	(0.001)	< 0.000	(0.001)	**0.002***	(0.001)
Variance Components: Random Effects											
Residual	σ^2	0.007	(0.001)	0.001	(< 0.001)	0.015	(0.002)	0.018	(0.002)	0.035	(0.004)
Intercept	τ_{00}	**0.028***	(0.003)	**0.011***	(0.001)	**0.090***	(0.007)	**0.073***	(0.008)	**0.122***	(0.013)

Parameter estimates from Model 3, the full model (standard errors in parentheses). * $p < 0.05$ corrected; † $p < 0.05$ uncorrected.

Table 3.6: Parameter estimates for relative power in posterior regions

3.6 Figures

Figure 3.1: Four regions-of-interest (ROI) were selected to provide spatial coverage over frontal (diamonds) and posterior (squares) portions of the scalp in the left (red) and right (blue) hemispheres. All ROIs contain 9 electrodes. The approximate 10-20 system electrode equivalents and the channel numbers for the regions are: ***F3*** *= 12, 18, 19, 20, 23, 24, 27, 28, 29;* ***F4*** *= 3, 4, 5, 10, 111, 117, 118, 123, 124;* ***P3*** *= 42, 47, 51, 52, 53, 59, 60, 61, 67; and* ***P4*** *= 77, 78, 85, 86, 91, 92, 93, 97, 98.*

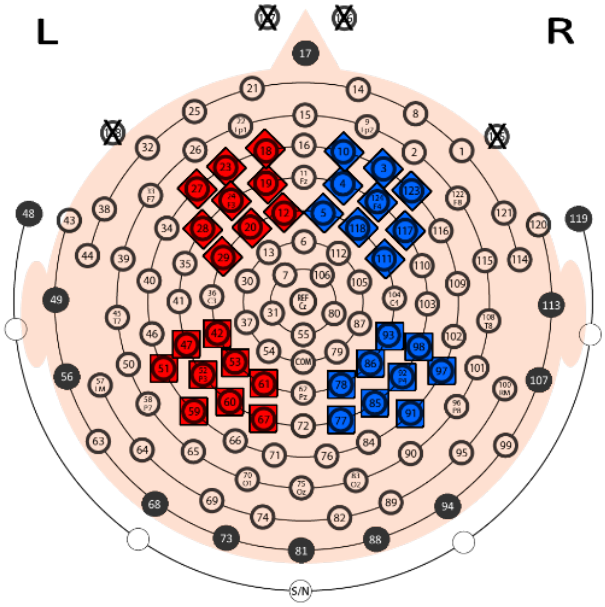

*Figure 3.2: Estimated marginal means of absolute power measures for the ASD (blue dotted line) and TD (solid red line groups). Separate graphs are plotted for frontal (top) and posterior (bottom) ROIs in the left and right hemispheres. Means were calculated using the full model (Eq 3). * $p < 0.05$ corrected, † $p < 0.05$ uncorrected.*

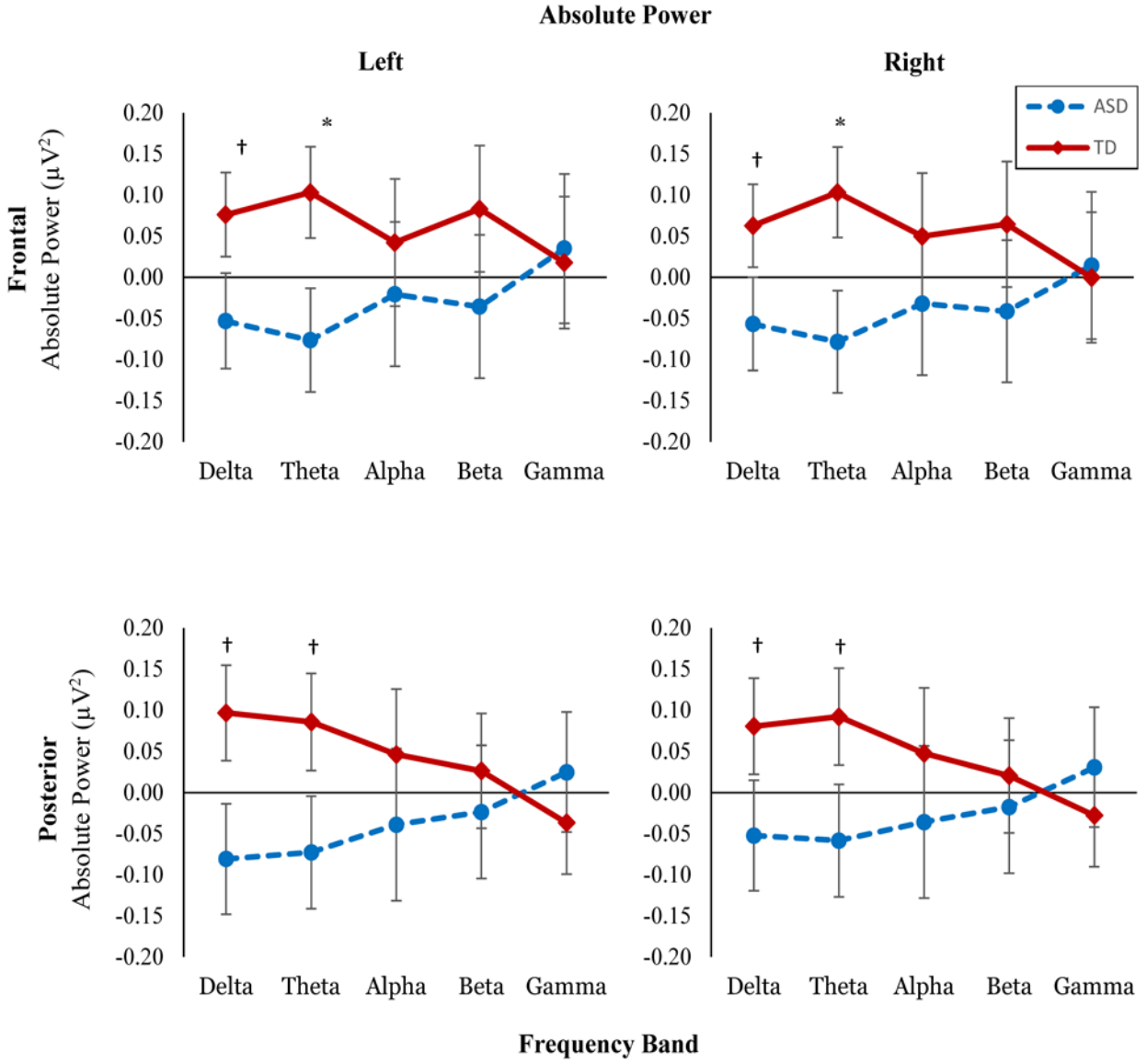

* $p < 0.05$ corrected, † $p < 0.05$ uncorrected.

References

Barry, R. J., Clarke, A. R., Hajos, M., McCarthy, R., Selikowitz, M., & Dupuy, F. E. (2010). Resting-state EEG gamma activity in children with attention-deficit/hyperactivity disorder. Clin Neurophysiol, 121(11), 1871-1877. doi: 10.1016/j.clinph.2010.04.022

Barry, R. J., Clarke, A. R., Johnstone, S. J., Magee, C. A., & Rushby, J. A. (2007). EEG differences between eyes-closed and eyes-open resting conditions. Clin Neurophysiol, 118(12), 2765-2773. doi: 10.1016/j.clinph.2007.07.028

Basar, E., Basar-Eroglu, C., Karakas, S., & Schurmann, M. (2000). Brain oscillations in perception and memory. Int J Psychophysiol, 35(2-3), 95-124.

Basar, E., Basar-Eroglu, C., Karakas, S., & Schurmann, M. (2001). Gamma, alpha, delta, and theta oscillations govern cognitive processes. Int J Psychophysiol, 39(2-3), 241-248.

Benninger, C., Matthis, P., & Scheffner, D. (1984). EEG development of healthy boys and girls. Results of a longitudinal study. Electroencephalogr Clin Neurophysiol, 57(1), 1-12.

Billeci, L., Sicca, F., Maharatna, K., Apicella, F., Narzisi, A., Campatelli, G., Muratori, F. (2013). On the application of quantitative EEG for characterizing autistic brain: a systematic review. Front Hum Neurosci, 7, 442. doi: 10.3389/fnhum.2013.00442

Bonfiglio, L., Olcese, U., Rossi, B., Frisoli, A., Arrighi, P., Greco, G., Carboncini, M. C. (2013). Cortical source of blink-related delta oscillations and their correlation with levels of consciousness. Hum Brain Mapp, 34(9), 2178-2189. doi: 10.1002/hbm.22056

Bonfiglio, L., Sello, S., Andre, P., Carboncini, M. C., Arrighi, P., & Rossi, B. (2009). Blink-related delta oscillations in the resting-state EEG: a wavelet analysis. Neurosci Lett, 449(1), 57-60. doi: 10.1016/j.neulet.2008.10.039

Bosl, W., Tierney, A., Tager-Flusberg, H., & Nelson, C. (2011). EEG complexity as a biomarker for autism spectrum disorder risk. BMC Med, 9, 18. doi: 10.1186/1741-7015-9-18

Cantor, D. S., & Chabot, R. (2009). QEEG studies in the assessment and treatment of childhood disorders. Clin EEG Neurosci, 40(2), 113-121.

Clarke, A. R., Barry, R. J., Dupuy, F. E., Heckel, L. D., McCarthy, R., Selikowitz, M., & Johnstone, S. J. (2011). Behavioural differences between EEG-defined subgroups of children with Attention-Deficit/Hyperactivity Disorder. Clin Neurophysiol, 122(7), 1333-1341. doi: 10.1016/j.clinph.2010.12.038

Croft, R. J., Chandler, J. S., Barry, R. J., Cooper, N. R., & Clarke, A. R. (2005). EOG correction: a comparison of four methods. Psychophysiology, 42(1), 16-24. doi: 10.1111/j.1468-8986.2005.00264.x

Dawson, G., Jones, E. J., Merkle, K., Venema, K., Lowy, R., Faja, S., Webb, S. J. (2012). Early behavioral intervention is associated with normalized brain activity in young children with autism. J Am Acad Child Adolesc Psychiatry, 51(11), 1150-1159. doi: 10.1016/j.jaac.2012.08.018

De Clercq, W., Vergult, A., Vanrumste, B., Van Paesschen, W., & Van Huffel, S. (2006). Canonical correlation analysis applied to remove muscle artifacts from the electroencephalogram. IEEE Trans Biomed Eng, 53(12 Pt 1), 2583-2587. doi: 10.1109/TBME.2006.879459

Deen, B., & Pelphrey, K. (2012). Perspective: Brain scans need a rethink. Nature, 491(7422), S20.

Delorme, A., & Makeig, S. (2004). EEGLAB: an open source toolbox for analysis of single-trial EEG dynamics including independent component analysis. J Neurosci Methods, 134(1), 9-21. doi: 10.1016/j.jneumeth.2003.10.009

Delorme, A., Sejnowski, T., & Makeig, S. (2007). Enhanced detection of artifacts in EEG data using higher-order statistics and independent component analysis. Neuroimage, 34(4), 1443-1449. doi: 10.1016/j.neuroimage.2006.11.004

Drongelen, W. v. (2007). Signal processing for neuroscientists : introduction to the analysis of physiological signals. Amsterdam ; Burlington, MA: Elsevier/Academic Press.

Elliott, C. D. (1993). Differential Abilities Scale (DAS). Child Assessment News, 3, 1-10.

Fatourechi, M., Bashashati, A., Ward, R. K., & Birch, G. E. (2007). EMG and EOG artifacts in brain computer interface systems: A survey. Clin Neurophysiol, 118(3), 480-494. doi: 10.1016/j.clinph.2006.10.019

Fletcher, E. M., Kussmaul, C. L., & Mangun, G. R. (1996). Estimation of interpolation errors in scalp topographic mapping. Electroencephalogr Clin Neurophysiol, 98(5), 422-434.

Freeman, W. J., Holmes, M. D., Burke, B. C., & Vanhatalo, S. (2003). Spatial spectra of scalp EEG and EMG from awake humans. Clinical Neurophysiology, 114(6), 1053-1068. doi: 10.1016/s1388-2457(03)00045-2

Gabard-Durnam, L., Tierney, A. L., Vogel-Farley, V., Tager-Flusberg, H., & Nelson, C. A. (2013). Alpha Asymmetry in Infants at Risk for Autism Spectrum Disorders. J Autism Dev Disord. doi: 10.1007/s10803-013-1926-4

Gasser, T., Sroka, L., & Mocks, J. (1985). The transfer of EOG activity into the EEG for eyes open and closed. Electroencephalogr Clin Neurophysiol, 61(2), 181-193.

Gasser, T., Sroka, L., & Mocks, J. (1986). The correction of EOG artifacts by frequency dependent and frequency independent methods. Psychophysiology, 23(6), 704-712.

Gmehlin, D., Thomas, C., Weisbrod, M., Walther, S., Pfuller, U., Resch, F., & Oelkers-Ax, R. (2011). Individual analysis of EEG background-activity within school age: impact of age and sex within a longitudinal data set. Int J Dev Neurosci, 29(2), 163-170. doi: 10.1016/j.ijdevneu.2010.11.005

Goncharova, I. I., McFarland, D. J., Vaughan, T. M., & Wolpaw, J. R. (2003). EMG contamination of EEG: spectral and topographical characteristics. Clinical Neurophysiology, 114(9), 1580-1593. doi: 10.1016/s1388-2457(03)00093-2

Gou, Z., Choudhury, N., & Benasich, A. A. (2011). Resting frontal gamma power at 16, 24 and 36 months predicts individual differences in language and cognition at 4 and 5 years. Behav Brain Res, 220(2), 263-270. doi: 10.1016/j.bbr.2011.01.048

Gratton, G., Coles, M. G., & Donchin, E. (1983). A new method for off-line removal of ocular artifact. Electroencephalogr Clin Neurophysiol, 55(4), 468-484.

Hagemann, D., Hewig, J., Walter, C., & Naumann, E. (2008). Skull thickness and magnitude of EEG alpha activity. Clin Neurophysiol, 119(6), 1271-1280. doi: 10.1016/j.clinph.2008.02.010

Hagemann, D., & Naumann, E. (2001). The effects of ocular artifacts on (lateralized) broadband power in the EEG. Clin Neurophysiol, 112(2), 215-231.

Hagemann, D., Naumann, E., Becker, G., Maier, S., & Bartussek, D. (1998). Frontal brain asymmetry and affective style: a conceptual replication. Psychophysiology, 35(4), 372-388.

Hoffmann, S., & Falkenstein, M. (2008). The correction of eye blink artefacts in the EEG: a comparison of two prominent methods. PLoS One, 3(8), e3004. doi: 10.1371/journal.pone.0003004

Iacono, W. G., & Lykken, D. T. (1981). Two-year retest stability of eye tracking performance and a comparison of electro-oculographic and infrared recording techniques: evidence of EEG in the electro-oculogram. Psychophysiology, 18(1), 49-55.

IBM Corp. Released 2012. IBM SPSS Statistics for Windows, Version 21.0. Armonk, NY: IBM Corp.

John, E. R., Ahn, H., Prichep, L., Trepetin, M., Brown, D., & Kaye, H. (1980). Developmental equations for the electroencephalogram. Science, 210(4475), 1255-1258.

Jung, T. P., Makeig, S., Humphries, C., Lee, T. W., McKeown, M. J., Iragui, V., & Sejnowski, T. J. (2000). Removing electroencephalographic artifacts by blind source separation. Psychophysiology, 37(2), 163-178.

Jung, T. P., Makeig, S., Westerfield, M., Townsend, J., Courchesne, E., & Sejnowski, T. J. (2000). Removal of eye activity artifacts from visual event-related potentials in normal and clinical subjects. Clin Neurophysiol, 111(10), 1745-1758.

Keil, A., Debener, S., Gratton, G., Junghofer, M., Kappenman, E. S., Luck, S. J., Yee, C. M. (2014). Committee report: Publication guidelines and recommendations for studies using electroencephalography and magnetoencephalography. Psychophysiology, 51(1), 1-21. doi: Doi 10.1111/Psyp.12147

Keren, A. S., Yuval-Greenberg, S., & Deouell, L. Y. (2010). Saccadic spike potentials in gamma-band EEG: characterization, detection and suppression. Neuroimage, 49(3), 2248-2263. doi: 10.1016/j.neuroimage.2009.10.057

Leuchter, A. F., Cook, I. A., Marangell, L. B., Gilmer, W. S., Burgoyne, K. S., Howland, R. H., Greenwald, S. (2009). Comparative effectiveness of biomarkers and clinical indicators for predicting outcomes of SSRI treatment in Major Depressive Disorder: results of the BRITE-MD study. Psychiatry Res, 169(2), 124-131. doi: 10.1016/j.psychres.2009.06.004

Luckhaus, C., Grass-Kapanke, B., Blaeser, I., Ihl, R., Supprian, T., Winterer, G., Brinkmeyer, J. (2008). Quantitative EEG in progressing vs stable mild cognitive impairment (MCI): results of a 1-year follow-up study. Int J Geriatr Psychiatry, 23(11), 1148-1155. doi: 10.1002/gps.2042

Ma, J., Tao, P., Bayram, S., & Svetnik, V. (2012). Muscle artifacts in multichannel EEG: characteristics and reduction. Clin Neurophysiol, 123(8), 1676-1686. doi: 10.1016/j.clinph.2011.11.083

Maguire, M. J., & Abel, A. D. (2013). What changes in neural oscillations can reveal about developmental cognitive neuroscience: language development as a case in point. Dev Cogn Neurosci, 6, 125-136. doi: 10.1016/j.dcn.2013.08.002

Marshall, P. J., Bar-Haim, Y., & Fox, N. A. (2002). Development of the EEG from 5 months to 4 years of age. Clin Neurophysiol, 113(8), 1199-1208.

McFarland, D. J., McCane, L. M., David, S. V., & Wolpaw, J. R. (1997). Spatial filter selection for EEG-based communication. Electroencephalogr Clin Neurophysiol, 103(3), 386-394.

McMenamin, B. W., Shackman, A. J., Greischar, L. L., & Davidson, R. J. (2011). Electromyogenic Artifacts and Electroencephalographic Inferences Revisited. Neuroimage, 54(1), 4-9. doi: 10.1016/j.neuroimage.2010.07.057

McMenamin, B. W., Shackman, A. J., Maxwell, J. S., Bachhuber, D. R., Koppenhaver, A. M., Greischar, L. L., & Davidson, R. J. (2010). Validation of ICA-based myogenic artifact correction for scalp and source-localized EEG. Neuroimage, 49(3), 2416-2432. doi: 10.1016/j.neuroimage.2009.10.010

McMenamin, B. W., Shackman, A. J., Maxwell, J. S., Greischar, L. L., & Davidson, R. J. (2009). Validation of regression-based myogenic correction techniques for scalp and source-localized EEG. Psychophysiology, 46(3), 578-592. doi: 10.1111/j.1469-8986.2009.00787.x

Monastra, V. J., Lubar, J. F., Linden, M., VanDeusen, P., Green, G., Wing, W., Fenger, T. N. (1999). Assessing attention deficit hyperactivity disorder via quantitative electroencephalography: an initial validation study. Neuropsychology, 13(3), 424-433.

Mullen, E. M. (1995). Mullen Scales of Early Learning: AGS Edition. Circle Pines, MN: American Guidance Service.

Napflin, M., Wildi, M., & Sarnthein, J. (2007). Test-retest reliability of resting EEG spectra validates a statistical signature of persons. Clin Neurophysiol, 118(11), 2519-2524. doi: 10.1016/j.clinph.2007.07.022

Niedermeyer, E., & Lopes da Silva, F. H. (2005). Electroencephalography : basic principles, clinical applications, and related fields (5th ed.). Philadelphia: Lippincott Williams & Wilkins.

Nunez, P. L., & Srinivasan, R. (2006). Electric fields of the brain : the neurophysics of EEG (2nd ed.). Oxford ; New York: Oxford University Press.

Nuwer, M. R. (2003). Clinical use of QEEG. Clin Neurophysiol, 114(12), 2225.

Oh, J., Han, M., Peterson, B. S., & Jeong, J. (2012). Spontaneous eyeblinks are correlated with responses during the Stroop task. PLoS One, 7(4), e34871. doi: 10.1371/journal.pone.0034871

Onton, J., Westerfield, M., Townsend, J., & Makeig, S. (2006). Imaging human EEG dynamics using independent component analysis. Neurosci Biobehav Rev, 30(6), 808-822. doi: 10.1016/j.neubiorev.2006.06.007

Perrin, F., Pernier, J., Bertrand, O., & Echallier, J. F. (1989). Spherical splines for scalp potential and current density mapping. Electroencephalogr Clin Neurophysiol, 72(2), 184-187.

Perrin, F., Pernier, J., Bertrand, O., Giard, M. H., & Echallier, J. F. (1987). Mapping of scalp potentials by surface spline interpolation. Electroencephalogr Clin Neurophysiol, 66(1), 75-81.

Picton, T. W., Bentin, S., Berg, P., Donchin, E., Hillyard, S. A., Johnson, R., Taylor, M. J. (2000). Guidelines for using human event-related potentials to study cognition: Recording standards and publication criteria. Psychophysiology, 37(2), 127-152. doi: Doi 10.1017/S0048577200000305

Pivik, R. T., Broughton, R. J., Coppola, R., Davidson, R. J., Fox, N., & Nuwer, M. R. (1993). Guidelines for the recording and quantitative analysis of electroencephalographic activity in research contexts. Psychophysiology, 30(6), 547-558.

Rabinoff, M., Kitchen, C. M., Cook, I. A., & Leuchter, A. F. (2011). Evaluation of quantitative EEG by classification and regression trees to characterize responders to antidepressant and placebo treatment. Open Med Inform J, 5, 1-8. doi: 10.2174/1874431101105010001

Raez, M. B., Hussain, M. S., & Mohd-Yasin, F. (2006). Techniques of EMG signal analysis: detection, processing, classification and applications. Biol Proced Online, 8, 11-35. doi: 10.1251/bpo115

Saby, J. N., & Marshall, P. J. (2012). The utility of EEG band power analysis in the study of infancy and early childhood. Dev Neuropsychol, 37(3), 253-273. doi: 10.1080/87565641.2011.614663

Satterthwaite, T. D., Wolf, D. H., Loughead, J., Ruparel, K., Elliott, M. A., Hakonarson, H., Gur, R. E. (2012). Impact of in-scanner head motion on multiple measures of functional connectivity: relevance for studies of neurodevelopment in youth. Neuroimage, 60(1), 623-632. doi: 10.1016/j.neuroimage.2011.12.063

Seifert, J., Naumann, E., Hewig, J., Hagemann, D., & Bartussek, D. (2006). Motivated executive attention--incentives and the noise-compatibility effect. Biol Psychol, 71(1), 80-89. doi: 10.1016/j.biopsycho.2005.03.001

Slifer, K. J., Avis, K. T., & Frutchey, R. A. (2008). Behavioral intervention to increase compliance with electroencephalographic procedures in children with developmental disabilities. Epilepsy Behav, 13(1), 189-195. doi: 10.1016/j.yebeh.2008.01.013

Snyder, S. M., & Hall, J. R. (2006). A meta-analysis of quantitative EEG power associated with attention-deficit hyperactivity disorder. J Clin Neurophysiol, 23(5), 440-455. doi: 10.1097/01.wnp.0000221363.12503.78

Sparrow, S. S., Cicchetti, D. V., & Balla, D. A. (2005). Vineland adaptive behavior scales (2nd ed.). Livonia, MN: Pearson Assessments.

Srinivasan, R., Nunez, P. L., Tucker, D. M., Silberstein, R. B., & Cadusch, P. J. (1996). Spatial sampling and filtering of EEG with spline laplacians to estimate cortical potentials. Brain Topogr, 8(4), 355-366.

Tager-Flusberg, H. Kasari, C. (2013). Minimally verbal school-aged children with autism spectrum disorder: the neglected end of the spectrum. Autism Res. 6(6):468-78

Takano, T. O., T. (1998). Characterization of developmental changes in EEG-gamma band activity during childhood using the autoregressive model.

Tierney, A. L., Gabard-Durnam, L., Vogel-Farley, V., Tager-Flusberg, H., & Nelson, C. A. (2012). Developmental trajectories of resting EEG power: an endophenotype of autism spectrum disorder. PLoS One, 7(6), e39127. doi: 10.1371/journal.pone.0039127

Uhlhaas, P. J., Roux, F., Rodriguez, E., Rotarska-Jagiela, A., & Singer, W. (2010). Neural synchrony and the development of cortical networks. Trends Cogn Sci, 14(2), 72-80. doi: 10.1016/j.tics.2009.12.002

Van Dijk, K. R., Sabuncu, M. R., & Buckner, R. L. (2012). The influence of head motion on intrinsic functional connectivity MRI. Neuroimage, 59(1), 431-438. doi: 10.1016/j.neuroimage.2011.07.044

van Tricht, M. J., Ruhrmann, S., Arns, M., Muller, R., Bodatsch, M., Velthorst, E., Nieman, D. H. (2014). Can quantitative EEG measures predict clinical outcome in subjects at Clinical High Risk for psychosis? A prospective multicenter study. Schizophr Res. doi: 10.1016/j.schres.2014.01.019

Wang, J., Barstein, J., Ethridge, L. E., Mosconi, M. W., Takarae, Y., & Sweeney, J. A. (2013). Resting state EEG abnormalities in autism spectrum disorders. J Neurodev Disord, 5(1), 24. doi: 10.1186/1866-1955-5-24

Webb, S. J., Bernier, R., Henderson, H. A., Johnson, M. H., Jones, E. J., Lerner, M. D., Westerfield, M. (2013). Guidelines and Best Practices for Electrophysiological Data Collection, Analysis and Reporting in Autism. J Autism Dev Disord. doi: 10.1007/s10803-013-1916-6

Whitham, E. M., Pope, K. J., Fitzgibbon, S. P., Lewis, T., Clark, C. R., Loveless, S., Willoughby, J. O. (2007). Scalp electrical recording during paralysis: quantitative evidence that EEG frequencies above 20 Hz are contaminated by EMG. Clin Neurophysiol, 118(8), 1877-1888. doi: 10.1016/j.clinph.2007.04.027

Yuval-Greenberg, S., & Deouell, L. Y. (2009). The broadband-transient induced gamma-band response in scalp EEG reflects the execution of saccades. Brain Topogr, 22(1), 3-6. doi: 10.1007/s10548-009-0077-6

Yuval-Greenberg, S., Tomer, O., Keren, A. S., Nelken, I., & Deouell, L. Y. (2008). Transient induced gamma-band response in EEG as a manifestation of miniature saccades. Neuron, 58(3), 429-441. doi: 10.1016/j.neuron.2008.03.027